TABLE 1. Summary of patients examined in the present study

Case	POR mutation	Skeletal anomaly	External genitalia	Other urogenital feature	Maternal virilization	Age at sampling of		Ref.
						24-h urine	Random spot urine	
Genetic male patients: 46,XY								
Group 1: two missense mutations								
1	R457H/R457H	Absent	Normal	IA	No		3 months, 12 months	7
2	R457H/R457H	Absent	Normal		Yes		22 yr	Unpublished
3	R457H/R457H	Absent	Normal		Yes		23 yr	Unpublished
Group 2: one missense and one other types of mutations								
4	R457H/Q201X	Overt	Normal		No		15 yr	Unpublished
5	R457H/Q201X	Overt	Normal		No		16 yr	Unpublished
6	R457H/A462_S463insIA	Overt	MP		Yes	3 months	10 d, 1 month, 2 months, 3 months (2×), 4 months (2×)	Unpublished
7	R457H/I444fsX449	Overt	Normal		No		14 yr (2×)	6
8	R457H/ L612_W620delinsR	Overt	MP, CO (R)		No		23 yr, 28 yr, 29 yr	4
9	R457H/ L612_W620delinsR	Overt	MP, HS, CO (L)	VUR (R)	No	18, 19, and 27 yr	23 yr, 25 yr, 26 yr (2×)	4
10	R457H/G5G[a]	Overt	CO (B)		No		17 yr	4
11	Y578C/I444fsX449	Overt	Normal		Yes		17 yr	4
Genetic female patients: 46,XX								
Group 1: two missense mutations								
12	R457H/R457H	Borderline	CM, LF (complete)	PCO (B)	Yes		1 month, 4 months	7
13	R457H/R457H	Borderline	CM, LF (complete)	PCO (B)	Yes		3 months, 4 months (2×)	7
14	R457H/R457H	Mild	CM, LF (complete)		Yes	2 yr	3 yr	4
15	R457H/R457H	Mild	CM, LF (complete)		No	8, 9, 10, and 11 yr	13 yr	4
16	R457H/R457H	Borderline	CM	VUR (B), PCO (L)	Yes		14 yr, 17yr	4
17	R457H/E580Q	Borderline	CM, LF (incomplete)		No		4 months, 8 months	Unpublished
Group 2: one missense and one other types of mutations								
18	R457H/IVS6+1G>A	Overt	CM, LF (complete)		Yes		5 yr	2
19	R457H/L565fsX574	Overt	CM, LF (complete)		Yes		10 yr	6
20	R457H/I444fsX449	Overt	CM, LF (complete)	PCO (L)	Yes	13 yr		4
21	R457H/Q201X	Overt	Normal		No		12 yr	Unpublished
22	R457H/?[b]	Overt	LF (partial)	VUR (R)	No		3 yr	4

MP, Micropenis; CO, cryptorchidism; HS, hypospadias; CM, clitoromegaly; LF, labial fusion; IA, imperforate anus; VUR, vesicoureteral reflux; PCO, polycystic ovary; R, right; L, left; B, bilateral. Cases 2, 3, and 16; cases 4, 5, and 21; and cases 8 and 9 are siblings.

[a] This silent substitution may affect pre-mRNA splicing.

[b] No mutation has been identified in one allele.

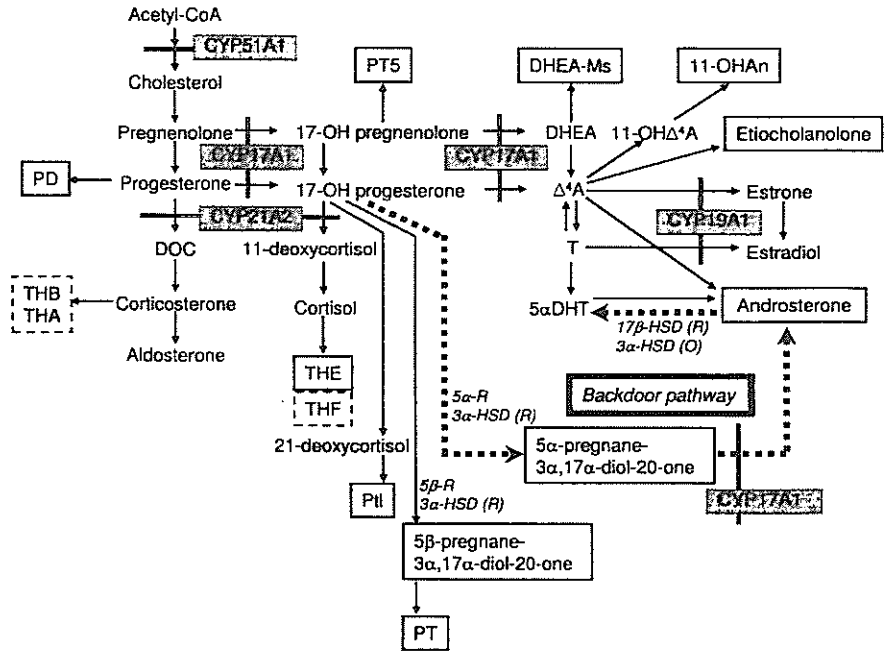

FIG. 1. Simplified schematic representation indicating the steroid metabolism pathway. CYP51A1 (lanosterol 14α-demethylase), CYP17A1 (17α-hydroxylase and 17,20 lyase), CYP21A2 (21-hydroxylase), and CYP19A1 (aromatase) are POR-dependent enzymes. The conventional frontdoor pathway is shown by the *solid lines* with *arrows*, and the alternative backdoor pathway is indicated by the *thick dotted lines* with *arrows*. In the backdoor pathway, the conversion of 17-OH progesterone into 5α-pregnane-3α,17α-diol-20-one is mediated by 5α-R (5α-reductase) and 3α-HSD (R) (reductive 3α-hydroxysteroid dehydrogenase), that of 5α-pregnane-3α,17α-diol-20-one into androsterone by CYP17A1 (17,20 lyase), and that of androsterone into DHT by 17β-HSD (R) (reductive 17β-hydroxysteroid dehydrogenase) and 3α-HSD (O) (oxidative 3α-hydroxysteroid dehydrogenase). 17-OH progesterone is also converted into 5β-pregnane-3α,17α-diol-20-one by 5β-reductase and 3α-HSD (R). Of the urine steroids analyzed in this study, those measurable since birth are surrounded by *solid squares*, and those measurable after 6 months of age are surrounded by *broken squares*. Note that androsterone can be derived from both the frontdoor and the backdoor pathways.

remained grossly normal in the PORD patients. By contrast, androsterone was increased during early infancy and remained grossly normal thereafter. Thus, despite the increased PT excretion, the androsterone to PT ratio remained normal during early infancy, although it decreased thereafter. Furthermore, the androsterone to etiocholanolone ratio tended to be increased during early infancy and remained grossly normal thereafter. 5α-Pregnane-3α,17α-diol-20-one was elevated throughout the examined ages, as was 5β-pregnane-3α,17α-diol-20-one.

Discussion

The urine steroid profile analysis revealed the combined CYP17A1 and CYP21A2 deficiency characteristic of PORD, in the conventional frontdoor pathway. Although several data may be confounding, they would not be inconsistent with PORD. For example, the normal THF and THE excretions would be explained as the consequence of steroidogenic adjustment to normalize the cortisol production under residual CYP17A1 and CYP21A2 activities and mild adrenocorticotropic hormone excess (2–7). Furthermore, because CYP21A2 is the sole POR-dependent enzyme involved in the mineralocorticoid biosynthesis, this would explain why THB and THA excretions tended to be increased in the presence of normal THF and THE excretions. In addition, because 17-OHP is markedly elevated, this would account for the normal PT to PD ratio and the normal to low-normal 11-OHAn and etiocholanolone excretions in the presence of residual CYP17A1 activity. Therefore, the results provide further support for the urine steroid profile analysis as a highly useful method for the diagnosis of PORD (4, 6, 7, 9, 16, 17).

Notably, urine androsterone excretion was elevated during early infancy in the PORD patients, despite the impaired CYP17A1 activity in the frontdoor pathway. By contrast, DHEA-Ms and 11-OHAn derived from the frontdoor pathway were at a low or low-normal range throughout the examined ages. Furthermore, etiocholanolone remained grossly normal throughout the examined ages including early infancy, and the androsterone to etiocholanolone ratio was elevated during early infancy. In this regard, of androsterone and etiocholanolone, which are considered to be net androgen Ms derived from both androgen precursors and active androgens, androsterone can be derived not only from the conventional frontdoor pathway via Δ^4A as well as DHT but also from the backdoor pathway via 5α-pregnane-3α,17α-diol-20-one, whereas etiocholanolone as well as DHEA-Ms and 11-OHAn should originate almost exclusively from the frontdoor pathway (9–13) (Fig. 1). Consistent with this, etiocholanolone remained grossly normal since birth, despite the elevation of 5β-pregnane-3α,17α-diol-20-one in our study. This suggests that etiocholanolone production in the backdoor route, *i.e.* the conversion of 5β-

TABLE 2. The number of urine samples obtained from control subjects

Age at sampling	24-h urine	First morning urine	Random spot urine	Total
Male				
0 ~ <1 month	0	0	366	366
1 month ~ <12 months	0	0	59	59
1 yr ~ <6 yr	9	0	39	48
6 yr ~ <12 yr	34	207	10	251
12 yr ~ <20 yr	40	59	0	99
20 yr ~ <30 yr	19	12	0	31
Total	102	278	474	854
Female				
0 ~ <1 month	0	0	311	311
1 month ~ <12 months	0	0	40	40
1 yr ~ <6 yr	7	0	9	16
6 yr ~ <12 yr	38	224	3	265
12 yr ~ <20 yr	45	84	0	129
20 yr ~ <30 yr	125	23	0	148
Total	215	331	363	909

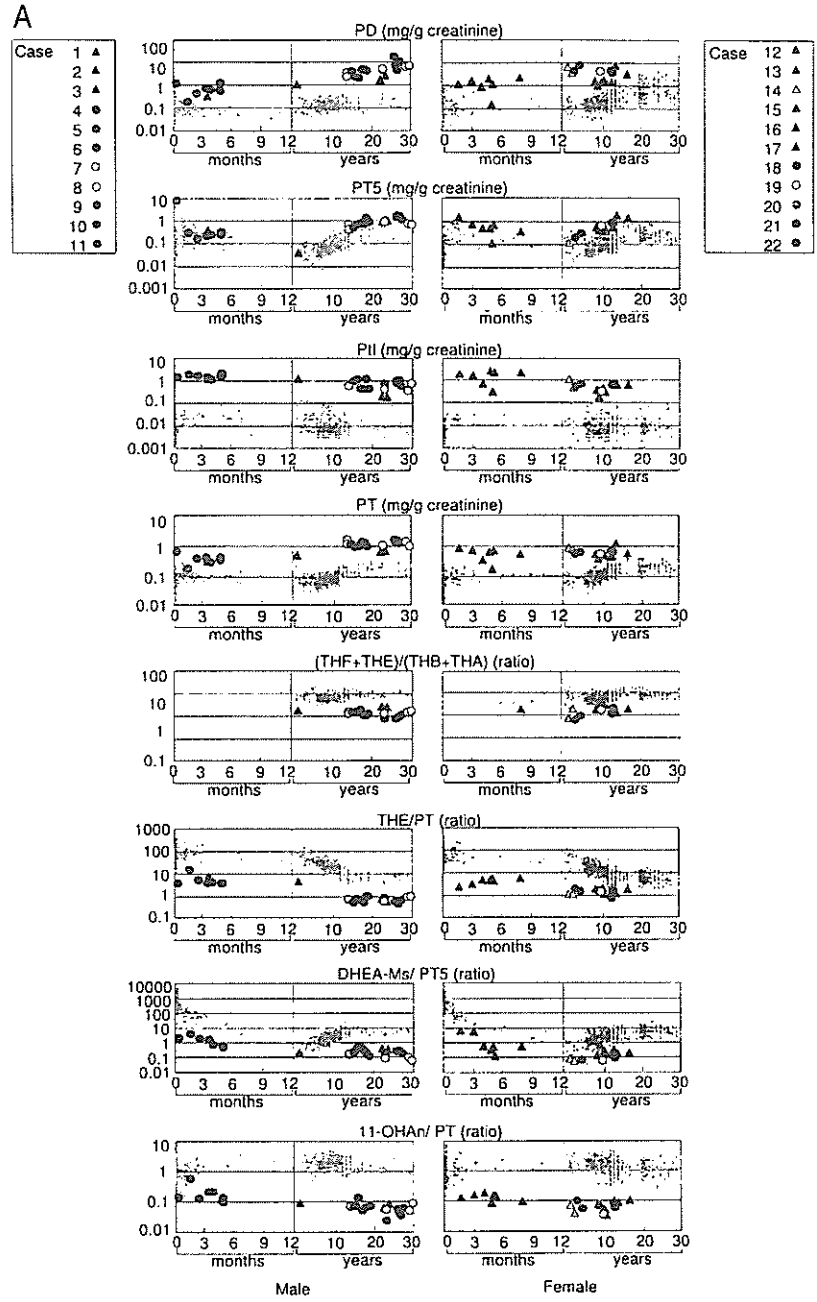

FIG. 2. Representative results of urine steroid profile analysis. A, The results for the assessment of the conventional frontdoor pathway. B, The results for the assessment of the alternative backdoor pathway. Cases 1–11 are genetic male patients, and cases 12–22 are genetic female patients. The *triangles* indicate group 1 patients with two missense mutations, and the *circles* represent group 2 patients with one missense and one non-missense mutation. Of the 22 cases, cases 1, 6, 12, 13, and 17 have been studied before 12 months of age, and the remaining 17 cases have been studied after 1 yr of age when the backdoor pathway is unlikely to exist. The *light blue circles* and the *pink circles* show the data obtained from 854 control males and 909 control females, respectively. Urine samples from the control subjects have been obtained before 12 months of age in 425 males and 351 females, and after 1 yr of age in the remaining 429 males and 558 females. Note that all the data are expressed using a logarithm scale except for the androsterone to etiocholanolone ratio that is expressed using a linear scale. (*Figure continues on next page.*)

pregnane-3α,17α-diol-20-one into etiocholanolone by CYP17A1, remains scanty, if any.

Thus, the transient increase in androsterone secretion during the first several months of life implies the operation of the backdoor pathway during this time period (10). Consistent with our results, Shackleton *et al.* (9) have identified the backdoor pathway-derived steroids, including androsterone, in the urine of the mother of a fetus with PORD. In this context, because androsterone is a potent androgen and an efficient DHT precursor, even a small excess would have clinical effects. Thus, even if the backdoor pathway is a quantitatively minor source of 19-carbon steroids relative to the frontdoor pathway, it would be relevant to the relatively well-preserved masculinization in genetic male patients and to the virilization in genetic female patients and in mothers of affected fetuses.

The backdoor pathway would primarily exist in the steroidogenic tissue(s) that transiently expresses several key enzymes including CYP17A1 and 5α-reductase to convert the accumulated 17-OHP into DHT (10) (Fig. 1). Thus, fetal to infantile gonads and/or adrenals would be the candidate tissue in the human (10). For the gonads, however, although steroidogenic cells are well developed in the fetal testis, they are barely present in the fetal to prepubertal ovary (18), yet the urine steroid profiles were similar between the male and female patients in this study. This may argue against the gonads being the major site for the backdoor pathway. For the adrenals, the fetal zone may be involved in the transient

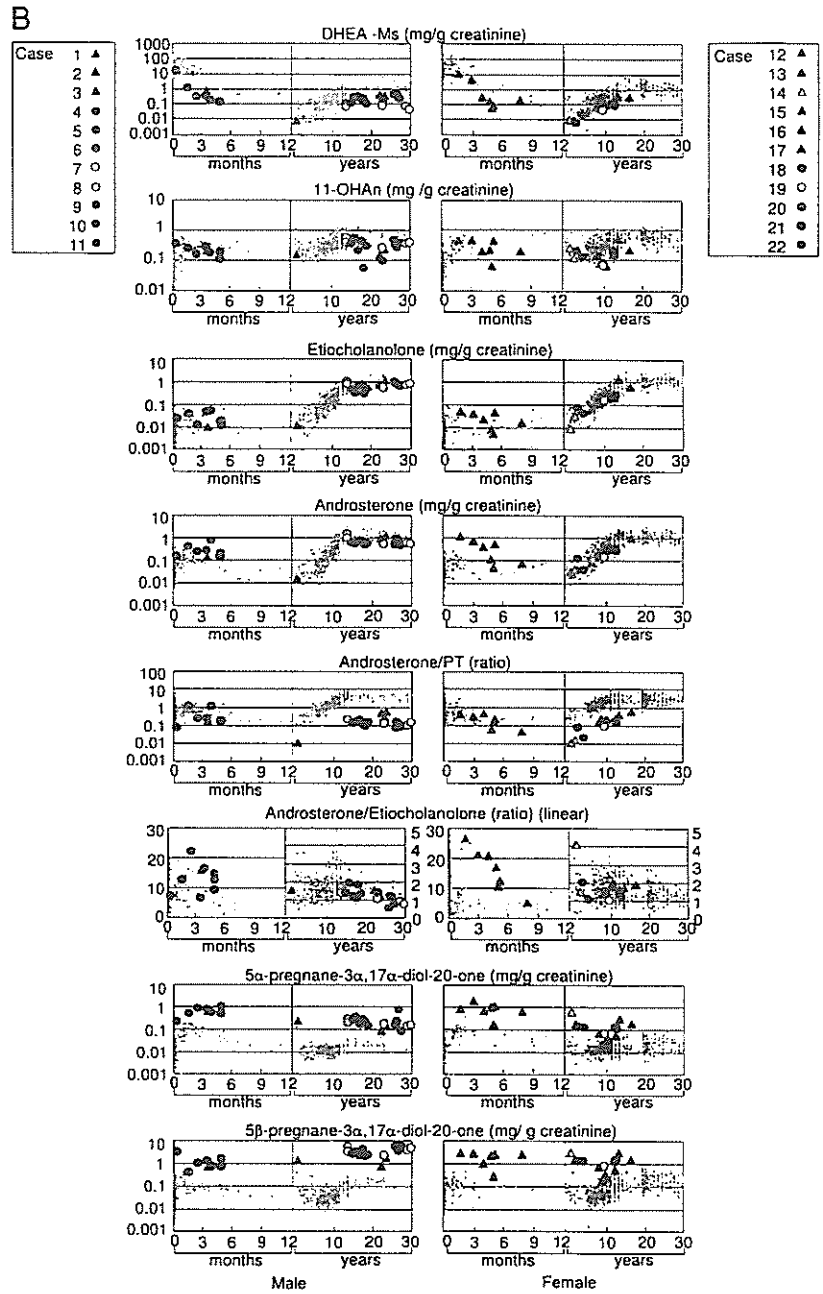

FIG. 2. *Continued*

activity of the backdoor pathway, because it disappears shortly after birth (19). In this context, because 3β-hydroxysteroid dehydrogenase activity is reduced in the fetal zone (19), it is unlikely that the fetal zone alone can produce a sufficient amount of 17-OHP to drive the backdoor pathway. However, because the fetal zone has abundant CYP17A1 activity (19), this may facilitate the conversion of the permanent zone derived 17-OHP into DHT via the backdoor pathway. In addition, other tissues/organs such as the fetal liver may also be relevant to the backdoor pathway. Therefore, this matter awaits further studies.

The urine steroid profile appeared grossly similar between groups 1 and 2. Thus, urine steroid profile analysis, although highly useful for the diagnosis of PORD, is unlikely to serve to differentiate between the two groups of PORD. This would be consistent with the extent of defective genital development of the patients and maternal virilization during pregnancy being similar between the two groups, although masculinization in genetic male patients tended to be better preserved in group 1 than in group 2 (Table 1). Indeed, the urine steroid profile and the total amount of androgens derived from the conventional frontdoor pathway, the backdoor pathway, and the placenta could be similar between the two groups, primarily because of the complexity of steroidogenesis in PORD (Fig. 1). For example, the amount of 17-OHP is determined by the balance between synthesis mediated by POR-dependent CYP17A1 and degradation mediated by POR-dependent CYP17A1 and CYP21A2, and such

enzymatic reactions would also depend on the amount of substrates and products as well as the residual enzyme activity. In this regard, because cholesterol production relevant to the development of skeletal lesion should be carried out in a simple manner (Fig. 1), this would explain why skeletal development was clearly different between groups 1 and 2. However, other genetic and/or environmental factors would also be relevant to the genital development, because case 21 with normal female genitalia had the similar steroid profile pattern.

Two points should be made with regard to the present study. First, urine steroid profile analysis was performed for random spot urine samples in most of the patients and for different types of urine samples in the control subjects, although random spot urine samples were primarily examined before 12 months of age in both the patients and the control subjects. This may have reduced the accuracy of the data, especially the excretion dosage data even after the correction with creatinine, because of the circadian rhythms of steroidogenesis. Second, urine steroid profile analysis in the early infantile period was carried out only in five cases, with repeated examinations in case 6, and most patients received the examinations at later age. Thus, further studies in the fetal-to-early-infantile period are necessary to provide more evidence for the presence of the backdoor pathway.

In summary, the results suggest that the backdoor pathway to DHT exists in the fetal-to-early-infantile period of PORD patients. Further studies will clarify the relevance of backdoor pathway to abnormal genital development in PORD as well as to virilization in 21-hydroxylase deficiency and other pathological conditions such as polycystic ovary syndrome.

Acknowledgments

Received November 10, 2005. Accepted April 3, 2006.

Address all correspondence and requests for reprints to: Dr. T. Ogata, Department of Endocrinology and Metabolism, National Research Institute for Child Health and Development, 2-10-1 Ohkura, Setagaya, Tokyo 157-8535, Japan. E-mail: tomogata@nch.go.jp.

This work was supported by a grant for Child Health and Development from the Ministry of Health, Labor, and Welfare (17C-2) and by a Grant-in-Aid for Scientific Research on Priority Areas from the Ministry of Education, Science, Sports and Culture (16086215).

The authors have nothing to declare.

References

1. **Miller WL** 2004 P450 oxidoreductase deficiency: a new disorder of steroidogenesis with multiple clinical manifestations. Trends Endocrinol Metab 15: 311–315
2. **Flück CE, Tajima T, Pandey AV, Arlt W, Okuhara K, Verge CF, Jabs EW, Mendonca BB, Fujieda K, Miller WL** 2004 Mutant P450 oxidoreductase causes disordered steroidogenesis with and without Antley-Bixler syndrome. Nat Genet 36:228–230
3. **Arlt W, Walker EA, Draper N, Ivison HE, Ride JP, Hammer F, Chalder SM, Borucka-Mankiewicz M, Hauffa BP, Malunowicz EM, Stewart PM, Shackleton CH** 2004 Congenital adrenal hyperplasia caused by mutant P450 oxidoreductase and human androgen synthesis: analytical study. Lancet 363: 2128–2135
4. **Fukami M, Horikawa R, Nagai T, Tanaka T, Naiki Y, Sato N, Okuyama T, Nakai H, Soneda S, Tachibana K, Matsuo N, Sato S, Homma K, Nishimura G, Hasegawa T, Ogata T** 2005 Cytochrome P450 oxidoreductase gene mutations and Antley-Bixler syndrome with abnormal genitalia and/or impaired steroidogenesis: molecular and clinical studies in 10 patients. J Clin Endocrinol Metab 90:414–426
5. **Huang N, Pandey AV, Agrawal V, Reardon W, Lapunzina PD, Mowat D, Jabs EW, Van Vliet G, Sack J, Fluck CE, Miller WL** 2005 Diversity and function of mutations in P450 oxidoreductase in patients with Antley-Bixler syndrome and disordered steroidogenesis. Am J Hum Genet 76:729–749
6. **Adachi M, Tachibana K, Asakura Y, Yamamoto T, Hanaki K, Oka A** 2004 Compound heterozygous mutations of cytochrome P450 oxidoreductase gene (POR) in two patients with Antley-Bixler syndrome. Am J Med Genet A 128:333–339
7. **Fukami M, Hasegawa T, Horikawa R, Ohashi T, Nishimura G, Homma K, Ogata T** 2006 Cytochrome P450 oxidoreductase deficiency in three patients initially regarded as having 21-hydroxylase deficiency and/or aromatase deficiency. Pediatr Res 59:276–280
8. **Grumbach MM, Auchus RJ** 1999 Estrogen: consequences and implications of human mutations in synthesis and action. J Clin Endocrinol Metab 84:4677–4694
9. **Shackleton C, Marcos J, Arlt W, Hauffa BP** 2004 Prenatal diagnosis of P450 oxidoreductase deficiency (ORD): a disorder causing low pregnancy estriol, maternal and fetal virilization, and the Antley-Bixler syndrome phenotype. Am J Med Genet A 129:105–112
10. **Auchus RJ** 2004 The backdoor pathway to dihydrotestosterone. Trends Endocrinol Metab 15:32–438
11. **Wilson JD, Auchus RJ, Leihy MW, Guryev OL, Estabrook RW, Osborn SM, Shaw G, Renfree MB** 2003 5α-Androstane-3α,17β-diol is formed in tammar wallaby pouch young testes by a pathway involving 5α-pregnane-3α,17α-diol-20-one as a key intermediate. Endocrinology 144:575–580
12. **Mahendroo M, Wilson JD, Richardson JA, Auchus RJ** 2004 Steroid 5α-reductase 1 promotes 5α-androstane-3α,17β-diol synthesis in immature mouse testes by two pathways. Mol Cell Endocrinol 222:113–120
13. **Gupta MK, Guryev OL, Auchus RJ** 2003 5α-Reduced C21 steroids are substrates for human cytochrome P450c17. Arch Biochem Biophys 418:151–160
14. **Homma K, Hasegawa T, Masumoto M, Takeshita E, Watanabe K, Chiba H, Kurosawa T, Takahashi T, Matsuo N** 2003 Reference values for urinary steroids in Japanese newborn infants: gas chromatography/mass spectrometry in selected ion monitoring. Endocr J 50:783–792
15. **Homma K, Hasegawa T, Takeshita E, Watanabe K, Anzo M, Toyoura T, Jinno K, Ohashi T, Hamajima T, Takahashi Y, Takahashi T, Matsuo N** 2004 Elevated urine pregnanetriolone definitively establishes the diagnosis of classical 21-hydroxylase deficiency in term and preterm neonates. J Clin Endocrinol Metab 89:6087–6091
16. **Cragun DL, Trumpy SK, Shackleton CH, Kelley RI, Leslie ND, Mulrooney NP, Hopkin RJ** 2004 Undetectable maternal serum uE3 and postnatal abnormal sterol and steroid metabolism in Antley-Bixler syndrome. Am J Med Genet A 129:1–7
17. **Shackleton C, Marcos J, Malunowicz EM, Szarras-Czapnik M, Jira P, Taylor NF, Murphy N, Crushell E, Gottschalk M, Hauffa B, Cragun DL, Hopkin RJ, Adachi M, Arlt W** 2004 Biochemical diagnosis of Antley-Bixler syndrome by steroid analysis. Am J Med Genet A 128:223–231
18. **Grumbach MM, Hughes IA, Conte FA** 2002 Disorders of sex differentiation. In: Larsen PR, Kronenberg HM, Melmed S, Polonsky KS, eds. Williams textbook of endocrinology. 10th ed. Philadelphia: Saunders; 842–1002
19. **Fusher DA** 2002 Endocrinology of fetal development. In: Larsen PR, Kronenberg HM, Melmed S, Polonsky KS, eds. Williams textbook of endocrinology. 10th ed. Philadelphia: Saunders; 811–841

JCEM is published monthly by The Endocrine Society (http://www.endo-society.org), the foremost professional society serving the endocrine community.

European Journal of Endocrinology (2007) 156 167–171 ISSN 0804-4643

CASE REPORT

Hypogonadotropic hypogonadism in an adult female with a heterozygous hypomorphic mutation of *SOX2*

Naoko Sato, Yusuke Kamachi[1], Hisato Kondoh[1], Yuichi Shima[2], Ken-ichirou Morohashi[2], Reiko Horikawa[3] and Tsutomu Ogata

Department of Endocrinology and Metabolism, National Research Institute for Child Health and Development, 2-10-1 Ohkura, Setagaya, Tokyo 157-8535, Japan, [1]Graduate School of Frontier Biosciences, Osaka University, Osaka, Japan, [2]Division of Cell Differentiation, National Institute for Basic Biology, Okazaki, Japan and [3]Division of Endocrinology and Metabolism, National Center for Child Health and Development, Tokyo, Japan

(Correspondence should be addressed to T Ogata; Email: tomogata@nch.go.jp)

Abstract

Objective: Heterozygous *SOX2* mutations have recently been reported to cause isolated hypogonadotropic hypogonadism (HH), in addition to ocular and brain abnormalities. Here, we report a further case with a heterozygous hypomorphic *SOX2* mutation and isolated HH.

Patient: The patient was a 28-year-old Japanese female with congenital right anophthalmia and poor pubertal development, who was found to have HH by a gonadotropin-releasing hormone test (peak serum LH, 2.3 mIU/ml; peak serum FSH, 2.9 mIU/ml). Other pituitary hormones were normal.

Methods: We performed mutation analysis of *SOX2* and functional studies of mutant SOX2 protein using the core enhancer sequence of the chicken δ-1-crystallin gene (*DC5*) and that of the mouse nestin gene (*Nes30*).

Results: A heterozygous missense mutation (224T>A, Leu75Gln) was identified in the DNA-binding domain. The mutant SOX2 protein had a severely reduced (approximately 10%) DNA-binding affinity and a markedly diminished (20–30%) transactivation potential with no dominant negative effect.

Conclusions: The results provide further support for the positive role of *SOX2* in the regulation of gonadotropin production.

European Journal of Endocrinology **156** 167–171

Introduction

Hypogonadotropic hypogonadism (HH) is a genetically heterogeneous condition defined by the deficiency of luteinizing hormone (LH) and follicle-stimulating hormone (FSH) secretion (1). It can occur as an isolated form or in association with other pituitary hormone deficiency. To date, several causative genes have been identified in isolated HH, including *GNRHR*, *GPR54*, *DAX1*, *SF-1*, *KAL1*, and *FGFR1* (2, 3). Of these, mutations of *GNRHR* and *GPR54* are free from clinical features other than isolated HH, whereas those of the remaining genes are usually associated with characteristic clinical phenotypes in addition to isolated HH (2, 3). However, mutations of such genes account for a relatively small fraction of patients with isolated HH (1), and underlying genetic factors remain to be elucidated in many patients with this condition.

SRY-related high mobility group (HMG) box gene 2 (*SOX2*) is a single exon gene encoding a member of SOX transcription factor family involved in the regulation of embryonic development and in the determination of cell fate (4–6). SOX proteins bind specific DNA sequences through their HMG domain, and regulate specific downstream target genes by interacting with a variety of partner proteins (6). *SOX2* is expressed in multiple developing tissues including the eyes and the central nervous system (CNS) (5, 7, 8), and paired box gene 6 and brain 2 act as partner proteins of SOX2 in transcriptional regulation during the lens and the CNS development respectively (8, 9). Consistent with this, heterozygous loss-of-function mutations of *SOX2* are known to cause ocular and CNS abnormalities (10, 11).

Recently, Kelberman *et al.* (12) have reported that heterozygous *SOX2* mutations cause anterior pituitary hypoplasia and apparently isolated HH. Six patients with functionally impaired *de novo* *SOX2* mutations invariably had HH, and exhibited clinical features consistent with HH such as micropenis and/or cryptorchidism in affected males and delayed or lack of pubertal development in affected females. Consistent with this, micropenis and/or cryptorchidism have previously been described in some male patients with *SOX2* mutations (10, 11).

However, there has been no other report documenting the association between a *SOX2* mutation and HH. Here, we report a further case with the association.

DOI: 10.1530/EJE-06-0606
Online version via www.eje-online.org

Subject and methods

Case report

This Japanese female patient was born at 36 weeks of gestation, with a birth length of 43.0 cm (−2.8 S.D.) and birth weight of 2.2 kg (−2.2 S.D.). She had congenital right anophthalmia, and received cosmetic repair with an artificial eye at 3 years of age. The non-consanguineous parents and the younger brother were clinically normal.

At 28 years of age she was referred to us, because of primary amenorrhea. Her height was 152.3 cm (−1.1 S.D.) and her weight 45.5 kg (−1.0 S.D.). Physical examination showed poor pubertal development (breast, Tanner stage 1; pubic hair, Tanner stage 2) with no virilization. Endocrine studies indicated isolated HH (Table 1), and her bone age was assessed as 15 years by the TW-2 method standardized for Japanese (15). Chromosome analysis revealed a 46,XX karyotype in all the 50 lymphocytes examined. Brain-computed tomography delineated right anophthalmia and apparently normal left eye and pituitary gland. The visual acuity of her left eye was 0.4 with a naked eye and 1.2 with a glass. Abdominal ultrasound studies indicated hypoplastic uterus and failed to detect ovaries. After consultation, she received oral hormone replacement therapy rather than gonadotropin therapy. She worked as a cook and had apparently normal mental development, although the measurement of intelligence quotient was refused.

Mutation analysis

This study was approved by the Institutional Review Board Committees at National Center for Child Health and Development and Osaka University. After obtaining written informed consent, leukocyte genomic DNA of this patient was amplified by PCR for the single coding exon and flanking UTRs of *SOX2*, using the primers shown in Table 2. Subsequently, the PCR products were subjected to direct sequencing on a CEQ 8000 autosequencer (Beckman Coulter, Fullerton, CA, USA). To confirm a heterozygous mutation, the corresponding PCR product was subcloned with TOPO TA Cloning Kit (Invitrogen), and normal and mutant alleles were sequenced separately. For controls, DNA samples of 100 normal individuals were utilized with permission.

DNA-binding assay

DNA-binding affinity of SOX2 HMG domain was examined for wildtype (WT) and mutant (MT) proteins using the core enhancer sequence at intron 3 of the chicken δ-1-crystallin gene (designated as DC5) harboring a SOX2 protein binding site (9). The detailed methods have been reported previously (9). In short, WT and MT SOX2 proteins (amino acids 2–184) tagged with 6xHis at the C-terminus were expressed in *Escherichia coli* as glutathione S-transferase (GST)-fusion proteins using expression vector pGEX-6P-1 (Amersham Pharmacia), and the GST tag was removed with PreScission protease. Varying amounts of the recombinant SOX2 proteins were incubated with the ^{32}P end-labeled DC5 and subjected to gel electrophoresis.

Transactivation analysis

Transactivation potential was examined with the Dual Luciferase Reporter Assay system (Promega), using DC5 containing the binding sites for SOX2 and chicken Pax6 proteins (9) and the core enhancer sequence at intron 2 of the mouse nestin gene (designated as Nes30) harboring the binding sites for SOX2 and mouse Brn2 proteins (8). The detailed methods were as described

Table 1 Summary of blood endocrine data.

	Patient data		Reference data	
	Baseline	Stimulated	Baseline	Stimulated
Luteinizing hormone (LH; mIU/ml)	<0.1	2.3[a]	1.8–7.6	8.5–15.5
Follicle-stimulating hormone (FSH; mIU/ml)	0.4	2.9[a]	5.2–14.4	8.3–20.0
Growth hormone (GH; ng/ml)	1.9	23.6[b]	0.6–3.5	>15.0
Adrenocorticotropic hormone (ACTH; pg/ml)	39	61[c]	9–52	>50
Thyroid-stimulating hormone (μU/ml)	0.6	14.8[d]	0.3–3.5	>10
Prolactin (ng/ml)	12.3	44.5[d]	1.5–15	5–70
Estradiol (pg/ml)	10	30[e]	20–120	300–1300
Testosterone (ng/ml)	<0.1	<0.1[f]	0.1–0.6	No female data
Insulin-like growth factor-I (ng/ml)	220	–	202–403	–
Cortisol (μg/dl)	18	22[g]	4–18	>20
Free thyroxine (pg/ml)	3.12	–	2.47–4.34	–
Free tri-iodothyronine (ng/dl)	1.56	–	0.97–1.79	–

Stimulated values represent (1) peak values during [a]a gonadotropin-releasing hormone test (100 μg bolus i.v), [b]a growth hormone-releasing hormone test (100 μg bolus i.v.), [c]a corticotropin-releasing hormone test (100 μg bolus i.v.), and [d]a thyrotropin-releasing hormone test (500 μg bolus i.v.) (blood sampling at 0, 30, 60, 90, and 120 min); (2) [e]the values after human menopausal gonadotropin stimulation (150 IU i.m. for 3 consecutive days) and [f]human chorionic gonadotropin stimulation (5000 IU i.m. for 3 consecutive days) (blood sampling on day 4); and (3) [g]the value after ACTH stimulation (250 μg i.v.) (blood sampling at 30 min). Reference data indicate the normal ranges in adult Japanese females (13, 14); those for LH and FSH indicate values at a follicular phase.

Table 2 The primer sequences and the PCR conditions utilized in the present study.

Primer	Forward primer; reverse primer	Location (bp)[a]	AT (C); PS (bp)
SOX2-1	CCGCATGTACAACATGATGGA; TTAGCCTCGTCGATGAACG	−4~+17; +266~+284	60; 288
SOX2-2	GAAACTTTTGTCGGAGACGGA; ATCATGCTGTAGCTGCCGTT	+237~+257; +502~+521	60; 285
SOX2-3	ACAGTTACGCGCACATGAA; ATGCTGATCATGTCCCGGA	+473~+491; +809~+827	60; 355
SOX2-4	ATGCACCGCTACGACGTGA; CCAAAAAGAAGTCCAGGATC	+589~+607; +1190~+1209	60; 621

AT, annealing temperature; PS, product size.
[a]The coding sequence for SOX2: +1~+951.

previously (8, 9). In brief, expression vectors for *SOX2* (WT and MT), chicken *Pax6*, and mouse *Brn2* were generated by inserting corresponding cDNAs into pCMV/SV2 vector (8), and luciferase reporter constructs were created by inserting DC5 and Nes30 into pδ51LucII vector with the δ1-crystallin promoter (8, 16). Subsequently, chicken embryo liver cells were transfected with (1) the reporter vector containing DC5 and the expression vectors for SOX2 (WT, MT, and WT plus MT) and Pax6, and (2) the reporter vector containing Nes30 and the expression vectors for SOX2 (WT, MT, and WT plus MT) and Brn2, together with phRG-TK vector (Promega) used as an internal control for the transfection. Luciferase assays (≥3 times) were performed at 48 h after the transfection.

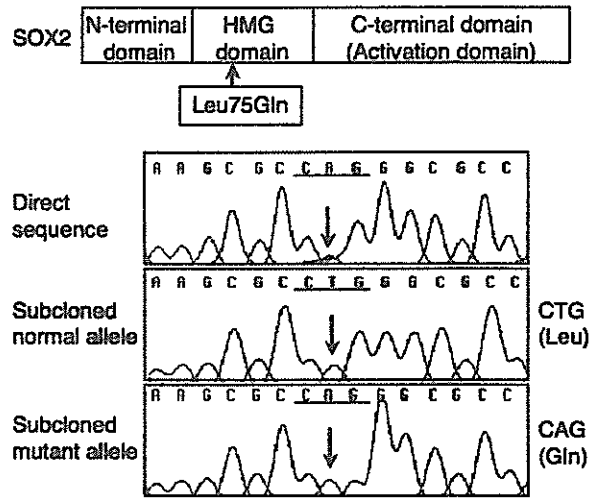

Figure 1 Mutation analysis of *SOX2* showing a heterozygous missense mutation (224T>A, L75Q). The mutation has been indicated by the direct sequencing, and confirmed by the subsequently performed sequencing of the subcloned normal and mutant alleles. The L75Q mutation resides at the HMG (high mobility group) domain with a DNA-binding capacity.

Results

Mutation analysis

A heterozygous transversion (224T>A) resulting in a substitution of the 75th leucine codon with a glutamine codon (L75Q) was identified in the helix II of DNA-binding HMG domain (Fig. 1). This missense mutation was absent in the 100 control subjects.

DNA-binding assay

The binding affinity of the MT SOX2 protein was severely reduced, as compared with that of the WT SOX2 protein (Fig. 2). Since 5 ng of the MT SOX2 protein gave similar intensity of the shifted band to 0.5 ng of the WT SOX2 protein, the DNA-binding affinity of the MT SOX2 protein was assessed as approximately 10% of that of the WT SOX2 protein.

Transactivation analysis

The transactivation potential of the MT SOX2 protein was markedly decreased, as compared with that of the WT SOX2 protein (approximately 20% for DC5 and approximately 30% for Nes30; Fig. 3A and B). Consistent with the severely attenuated (approximately 10%) DNA-binding affinity, the activation levels were similar between the assays using 2 ng of the MT SOX2 expression vector and those using 0.2 ng of the WT SOX2 expression vector, for both reporters with DC5 and Nes30. Furthermore, the activation levels were comparable between the assays with WT SOX2 protein only and those with WT plus MT SOX2 proteins for both reporters, indicating the lack of a dominant negative effect of the MT SOX2 protein.

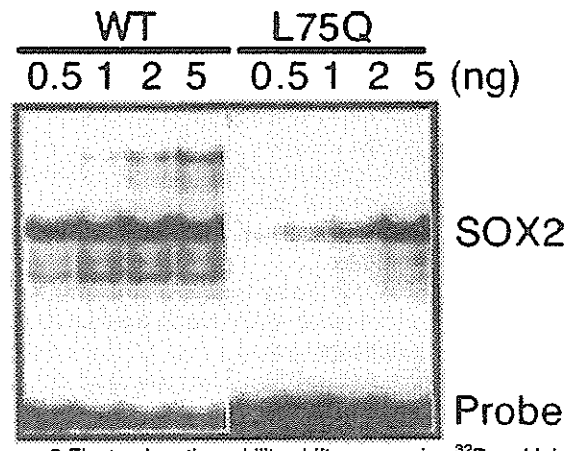

Figure 2 Electrophoretic mobility shift assay using ^{32}P end-labeled DC5 and the wildtype (WT) and the L75Q mutant SOX2 proteins.

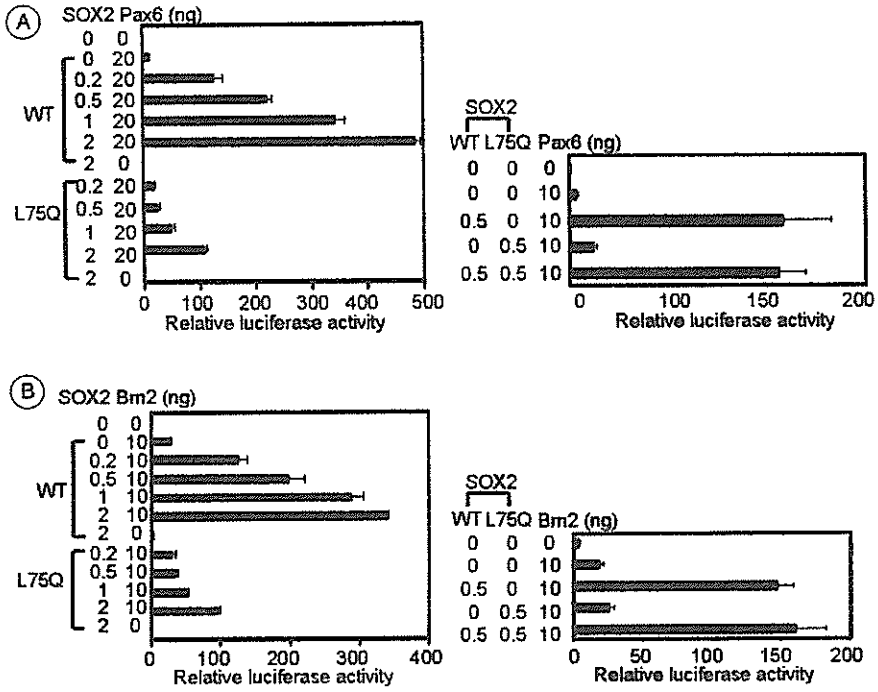

Figure 3 Transactivation function of the wildtype (WT) and the L75Q mutant SOX2 proteins for DC5 (A) and Nes30 (B). Relative luciferase activities are shown with the mean and the S.D., with an activity generated by the reporter lacking DC5 or Nes30 being taken as 1.

Discussion

A heterozygous L75Q mutation was identified in the HMG domain of *SOX2* in this patient. Furthermore, the MT SOX2 protein was shown to have reduced DNA-binding affinity and decreased transcription activity with no dominant negative effect. These findings suggest that the L75Q mutation is a hypomorphic mutation retaining a residual activity.

This patient had unilateral anophthalmia and apparently normal mental development. This mild phenotype would primarily be due to the residual SOX2 activity. In addition, other genetic and environmental factors would also be relevant to the phenotypic consequences, because the ocular and CNS phenotype is not necessarily dependent on the residual activity alone (12). Furthermore, the degree of residual SOX2 activity and the status of other factors would also be involved in the development of several infrequent features such as esophageal atresia, sensorineural deafness, and short stature (10–12, 17, 18).

The salient feature of this patient is isolated HH. This provides further support for *SOX2* being involved in the regulation of gonadotropin production. In this context, several findings are noteworthy. First, she had obvious HH in the presence of relatively mild ocular lesion and apparently normal CNS function. This would primarily be compatible with the phenotype of heterozygous *Sox2* knockout mice exhibiting pituitary dysfunction and normal ocular development (12), and may suggest that gonadotropin production is more sensitive to the reduced SOX2 function than ocular and CNS development. Second, there was no anterior pituitary hypoplasia. This implies that *SOX2* mutations do not necessarily lead to pituitary hypoplasia. Third, other pituitary hormones were normal, as in the patients described by Kelberman *et al.* (12). This suggests that the gonadotropin is most vulnerable to reduced *SOX2* dosage among pituitary hormones. However, it should be pointed out that heterozygous *Sox2* knockout mice have multiple pituitary hormone deficiency (12), and that SOX2 protein is capable of transactivating *HESX1* (12, 19), a causative gene for panhypopituitarism and optic nerve abnormality (20). Thus, in conjunction with anterior pituitary hypoplasia in most patients with *SOX2* mutations (12), heterozygous *SOX2* mutations could affect other pituitary hormones in exceptional patients.

It remains to be clarified how *SOX2* mutations lead to HH. However, it has been reported that murine *Sox2* expression is identified in the presumptive hypothalamus and the Rathke's pouch at E11.5, whereas it is confined around the Rathke's pouch lumen at a later age and detected in some non-endocrine cells only in the adult pituitary (12). Thus, HH in *SOX2* mutations may primarily be ascribed to dysregulated hypothalamopituitary axis during the early life, rather than a cell-type specific dysfunction of the gonadotropes.

In summary, the results provide further support for the positive role of *SOX2* in the regulation of gonadotropin production. Further studies will permit to define the pituitary phenotype and the molecular mechanism leading to HH in patients with *SOX* mutations.

Acknowledgements

This work was supported in part by grants for Child Health and Development (17C-2) and for Research on Children and Families from the Ministry of Health, Labor, and Welfare, and by a Grant-in-Aid for Scientific Research on Priority Areas (16086215) and Category S (17107005) from the Ministry of Education, Science, Sports and Culture.

References

1 Grumbach MM & Styne DM. Puberty: ontogeny, neuroendocrinology, physiology, and disorders. In *Williams Textbook of Endocrinology*, edn 10, pp 1115–1286. Eds PR Larsen, HM Kronenberg, S Melmed & KS Polonsky. Philadelphia: Saunders, 2002.

2 Iovane A, Aumas C & de Roux N. New insights in the genetics of isolated hypogonadotropic hypogonadism. *European Journal of Endocrinology* 2004 **151** 83–88.

3 Achermann JC, Ozisik G, Meeks JJ & Jameson JL. Genetic causes of human reproductive disease. *Journal of Clinical Endocrinology and Metabolism* 2002 **87** 2447–2454.

4 Kamachi Y, Uchikawa M & Kondoh H. Pairing SOX off: with partners in the regulation of embryonic development. *Trends in Genetics* 2000 **16** 182–187.

5 Avilion AA, Nicolis SK, Pevny LH, Perez L, Vivian N & Lovell-Badge R. Multipotent cell lineages in early mouse development depend on SOX2 function. *Genes and Development* 2003 **17** 126–140.

6 Kondoh H, Uchikawa M & Kamachi Y. Interplay of Pax6 and SOX2 in lens development as a paradigm of genetic switch mechanisms for cell differentiation. *International Journal of Developmental Biology* 2004 **48** 819–827.

7 Kamachi Y, Sockanathan S, Liu Q, Breitman M, Lovell-Badge R & Kondoh H. Involvement of SOX proteins in lens-specific activation of crystallin genes. *EMBO Journal* 1995 **14** 3510–3519.

8 Tanaka S, Kamachi Y, Tanouchi A, Hamada H, Jing N & Kondoh H. Interplay of SOX and POU factors in regulation of the Nestin gene in neural primordial cells. *Molecular and Cellular Biology* 2004 **24** 8834–8846.

9 Kamachi Y, Uchikawa M, Tanouchi A, Sekido R & Kondoh H. Pax6 and SOX2 form a co-DNA-binding partner complex that regulates initiation of lens development. *Genes and Development* 2001 **15** 1272–1286.

10 Fantes J, Ragge NK, Lynch SA, McGill NI, Collin JR, Howard-Peebles PN, Hayward C, Vivian AJ, Williamson K, van Heyningen V & Fitzpatrick DR. Mutations in SOX2 cause anophthalmia. *Nature Genetics* 2003 **33** 461–463.

11 Ragge NK, Lorenz B, Schneider A, Bushby K, de Sanctis L, de Sanctis U, Salt A, Collin JR, Vivian AJ, Free SL, Thompson P, Williamson KA, Sisodiya SM, van Heyningen V & Fitzpatrick DR. SOX2 anophthalmia syndrome. *American Journal of Medical Genetics Part A* 2005 **135** 1–7.

12 Kelberman D, Rizzoti K, Avilion A, Bitner-Glindzicz M, Cianfarani S, Collins J, Chong WK, Kirk JM, Achermann JC, Ross R, Carmignac D, Lovell-Badge R, Robinson IC & Dattani MT. Mutations within Sox2/SOX2 are associated with abnormalities in the hypothalamo–pituitary–gonadal axis in mice and humans. *Journal of Clinical Investigation* 2006 **116** 2442–2455.

13 Japan Public Health Association. *Normal Biochemical Values in Japanese Children*. Tokyo: Sanko Press, 1996 (in Japanese).

14 Ujihara M. Normal blood and urine hormone values in the Japanese. In *Manual for Diagnosis and Treatment of Endocrine Disorders*, pp 177–187. Eds K Shizume & K Takano. Tokyo: Igaku-no-Sekai-sha, 1997 (in Japanese).

15 Murata M, Matsuo N, Tanaka T, Ohtsuki F, Ashizawa K, Tatara H, Anzo M, Sato M, Matsuoka H, Asami T & Tsukakoshi K. *Radiographic Atlas of Skeletal Development for the Japanese*. Tokyo: Kanehara Press, 1993 (in Japanese).

16 Kamachi Y & Kondoh H. Overlapping positive and negative regulatory elements determine lens-specific activity of the delta 1-crystallin enhancer. *Molecular and Cellular Biology* 1993 **13** 5206–5215.

17 Williamson KA, Hever AM, Rainger J, Rogers RC, Magee A, Fiedler Z, Keng WT, Sharkey FH, McGill N, Hill CJ, Schneider A, Messina M, Turnpenny PD, Fantes JA, van Heyningen V & Fitzpatrick DR. Mutations in SOX2 cause anophthalmia–esophageal–genital (AEG) syndrome. *Human Molecular Genetics* 2006 **15** 1413–1422.

18 Hagstrom SA, Pauer GJ, Reid J, Simpson E, Crowe S, Maumenee IH & Traboulsi EI. SOX2 mutation causes anophthalmia, hearing loss, and brain anomalies. *American Journal of Medical Genetics Part A* 2005 **138** 95–98.

19 Eroshkin F, Kazanskaya O, Martynova N & Zaraisky A. Characterization of cis-regulatory elements of the homeobox gene Xanf-1. *Gene* 2002 **285** 279–286.

20 Dattani MT, Martinez-Barbera JP, Thomas PQ, Brickman JM, Gupta R, Martensson IL, Toresson H, Fox M, Wales JK, Hindmarsh PC, Krauss S, Beddington RS & Robinson IC. Mutations in the homeobox gene HESX1/Hesx1 associated with septo-optic dysplasia in human and mouse. *Nature Genetics* 1998 **19** 125–133.

Received 23 November 2006
Accepted 27 November 2006

0021-972X/06/$15.00/0
Printed in U.S.A.

The Journal of Clinical Endocrinology & Metabolism 91(4):1415–1418

doi: 10.1210/jc.2005-2266

BRIEF REPORT

Kallmann Syndrome: Somatic and Germline Mutations of the Fibroblast Growth Factor Receptor 1 Gene in a Mother and the Son

Naoko Sato, Kenji Ohyama, Maki Fukami, Michiyo Okada, and Tsutomu Ogata

Department of Endocrinology and Metabolism, National Research Institute for Child Health and Development (N.S., M.F., M.O., T.O.), Tokyo 157-8535, Japan; and Interdisciplinary Graduate School of Medicine and Engineering Sciences, University of Yamanashi (K.O.), Yamanashi 409-3898, Japan

Context: Although Kallmann syndrome (KS) caused by heterozygous loss of function mutations of the fibroblast growth factor receptor 1 gene (*FGFR1*) is occasionally associated with characteristic features, such as dental agenesis and cleft palate, *FGFR1* mutations remain unidentified in several KS patients with such characteristic features.

Subjects and Methods: We examined a 14-yr-old Japanese boy with hypogonadotropic hypogonadism, olfactory dysfunction, and dental agenesis and his fertile mother with olfactory dysfunction and dental agenesis. Direct sequencing was performed for *FGFR1* using leukocyte genomic DNA from the proband and leukocyte and nail genomic DNA from the mother. To examine a possible somatic mutation, a specific forward primer was designed to introduce a *Bst*XI site into the normal allele only, and nested PCR amplification, followed by *Bst*XI digestion, was carried out three times with different reverse primers.

Results: After standard PCR amplifications, a heterozygous 2-bp deletion at exon 10 (1317_1318delTG), which is predicted to cause a frameshift at the 439th codon for serine and resultant termination at the 461st codon (S439fsX461), was identified in the proband, but was not found in the mother. After selective amplification of the mutant allele, this deletion was detected in nail DNA, but not in leukocyte DNA, from the mother.

Conclusion: The results suggest that the 2-bp deletion took place as a somatic mutation in the mother and was transmitted to the boy because of germline mosaicism. Such a somatic mutation occurs in some apparently *FGFR1* mutation-negative KS patients with dental agenesis. (***J Clin Endocrinol Metab* 91: 1415–1418, 2006**)

KALLMANN SYNDROME (KS) is a congenital developmental disorder defined by the combination of hypogonadotropic hypogonadism (HH) and anosmia/hyposmia (1). To date, two genes have been identified for KS, *i.e. KAL1* (Kallmann syndrome 1) on Xp22.3 for the X-linked form (2, 3) and *FGFR1* (fibroblast growth factor receptor 1, also known as *KAL2*) on 8p12 for one autosomal dominant form (4). For *FGFR1*, it has been shown that heterozygous loss of function mutations account for approximately 10% of KS patients, and that the clinical spectrum in mutation-positive patients ranges widely from the typical KS phenotype to an apparently normal phenotype with fertility (4–7). In addition, such patients occasionally show characteristic features such as cleft palate and dental agenesis (4, 6, 7).

A gene mutation can take place during somatic cell division in addition to the gametogenic process (8). This results in somatic mosaicism that can lead to various degrees of clinical phenotype relevant to the mutation depending on the distribution and frequency of the mutation-positive somatic cells in an affected individual. Furthermore, if the somatic mutation occurs at an early stage before the separation of germline cells from somatic cells, it can be transmitted to the offspring in its complete form because of germline mosaicism (8). In this study we report on a Japanese family in which a maternal somatic mutation of *FGFR1* was transmitted to her son as a germline mutation.

Patients and Methods

The proband of this family was a boy who was referred to Yamanashi University Hospital because of lack of pubertal development at 14 yr and 9 months of age. He exhibited a eunuchoid habitus with no pubertal development (pubic hair, Tanner stage 1; genitalia, Tanner stage 1). The penis was 2.8 cm long, and the testes were 2 ml in volume and palpable within the scrotum bilaterally. His height was 145.6 cm (−1.8 SD), and his weight was 57.8 kg (+0.2 SD). The annual growth data obtained at school indicated that his height remained around −0.2 SD in childhood and gradually decreased to −1.8 SD because of no pubertal growth spurt. His bone age was assessed as 12.5 yr by the TW-2 method standardized for the Japanese. A GnRH test (100 $\mu g/m^2$ bolus iv; blood sampling at 0, 30, 60, 90, and 120 min) showed grossly age-appropriate serum gonadotropin values [basal LH, 0.7 IU/liter (normal range, 1.5–6.0 IU/liter); peak LH, 9.4 IU/liter (5.7–18.5 IU/liter); basal FSH, 2.9 IU/liter (1.5–6.0 IU/liter); peak FSH, 11.0 IU/liter (7.0–14.0 IU/liter)], whereas a human chorionic gonadotropin test (3000 IU/m^2/dose, im, for 3 consecutive days; blood sampling on d 1–4) revealed a severely compromised serum basal testosterone (T) value [7.8 ng/dl (0.2 nmol/liter); normal range, 100–600 ng/dl (3.4–20.8 nmol/liter)] and subnormal T response [225 ng/dl (7.8 nmol/liter); >300 ng/dl (>10.4 nmol/liter)]. Furthermore, he had no sense of smell, and magnetic resonance imaging

First Published Online January 17, 2006

Abbreviations: FGFR1, Fibroblast growth factor receptor 1; HH, hypogonadotropic hypogonadism; KS, Kallmann syndrome; T, testosterone.

delineated mildly hypoplastic olfactory bulbs. Thus, he was diagnosed as having KS. He also had agenesis of eight teeth (first upper and lower molars, upper premolar teeth, and lower canine teeth), although he was free from other features reported in KS, such as mirror movement, renal aplasia, cleft palate, high arched palate, and perceptive deafness. He was treated with T enanthate (125 mg/month, im) from 15 yr and 4 months of age. On the last examination at 17 yr and 7 months of age, he was 169.3 cm in height (−0.2 SD) and 63.4 kg in weight (+0.2 SD), and manifested secondary sexual development (pubic hair, Tanner stage 4; genitalia, Tanner stage 3), although his testes remained 2 ml in volume bilaterally.

The 47-yr-old mother also lacked a sense of smell and had agenesis of six teeth (first upper and lower molars and lower canine teeth). She had normal stature (160.0 cm; +0.4 SD) and exhibited full secondary sexual development. In the follicular phase, basal serum LH was 3.1 IU/liter (normal range, 1.8–7.6 IU/liter), FSH was 3.7 IU/liter (normal range, 5.2–14.4 IU/liter), and estradiol was 70.1 pg/ml [257 pmol/liter; normal range, 20–120 pg/ml (73.4–440 pmol/liter)]. Her menarche occurred at 13.6 yr of age (normal range, 9.75–14.75 yr) and was followed by regular menses of 34-day cycles (normal cycle periods, 24–35 d) (9). She gave birth to four children after uncomplicated term pregnancies and deliveries and fed them with artificial milk. Her menses resumed more than 1 yr after each delivery, although menses usually resume at approximately 6 wk postpartum in nonbreast feeding women (10). However, no data were available for factors influencing the postpartum amenorrheic periods, such as the postpartum weight change, the degree of exercise, and the pituitary-gonadal function status.

The father and the three children (a 20-yr-old boy, a 16-yr-old boy, and a 13-yr-old girl) had age-appropriate secondary sexual development and normal sense of smell. Furthermore, dental examination showed no abnormality in the four family members. Allegedly, the maternal parents also had no discernible abnormal features.

Molecular analysis of FGFR1

This study has been approved by the institutional review board committee at the National Center for Child Health and Development. After obtaining written informed consent, leukocyte genomic DNA of the proband and the mother was PCR amplified for the coding exons of *FGFR1* (exons 2–18), and the PCR products were subjected to direct sequencing from both directions on a CEQ 8000 autosequencer (Beckman Coulter, Fullerton, CA). The primer sequences and PCR conditions have been described previously (5). Consequently, a heterozygous 2-bp deletion at exon 10 (1317_1318delTG), which is predicted to cause a frameshift at the 439th codon for serine and resultant termination at the 461st codon (S439fsX461), was identified in the proband (Fig. 1A). This mutation was confirmed by sequencing the subcloned normal and mutant alleles (TOPO TA Cloning Kit, Invitrogen Life Technologies, Inc., Carlsbad, CA). By contrast, this 2-bp deletion was not detected in the mother (Fig. 1B).

Thus, the possibility of a somatic mutation was examined in the mother. For this purpose, approximately 1.3 μg of genomic DNA was extracted from the 10 fingernails that were left uncut for two wk, using SMITEST EX-R&D kit (Genome Science Laboratories Co., Ltd., Fukushima, Japan) (11). To avoid contamination of the proband's tissue such as a piece of nail trapped in the nail cutter or skin scratched by the maternal nails, the maternal nails were obtained with a new nail cutter after careful washing with a brush at the Hospital. Then, 0.1 μg of nail genomic DNA was amplified for the region harboring the 2-bp deletion mutation by PCR of 35 cycles, with equipments that were never used for the DNA analysis of the proband, to avoid contamination of the proband's DNA. Direct sequencing of the PCR products, however, failed to detect the mutation.

Next, a selective amplification of the mutant allele was attempted for

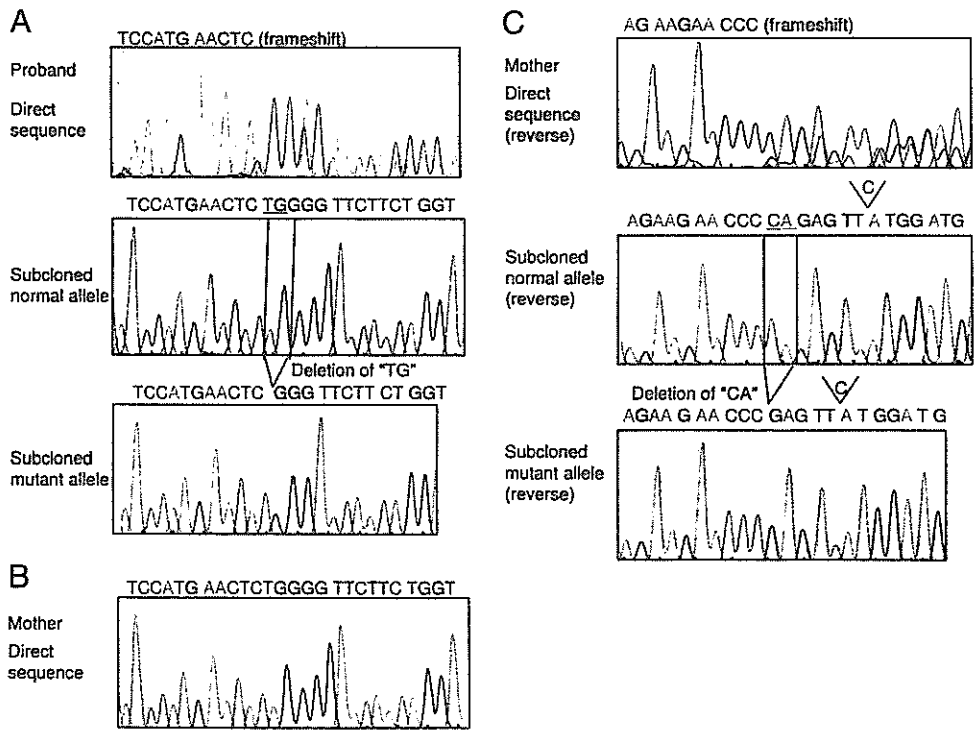

FIG. 1. Sequence analysis of *FGFR1* in the proband and the mother. A, Electrochromatograms obtained by the standard amplification for the leukocyte genomic DNA of the proband. A heterozygous 2-bp deletion at exon 10 (1317_1318delTG) has been indicated by the direct sequencing, and confirmed by the subsequent sequencing of the subcloned normal and mutant alleles. This mutation is predicted to cause a frameshift at the 439th codon for serine and resultant termination at the 461st codon (S439fsX461). B, An electrochromatogram obtained by the standard amplification for the leukocyte genomic DNA of the mother. The nucleotide sequence is normal with no trace of the 2-bp deletion mutation identified in the proband. C, Electrochromatograms obtained by the selective amplification of the mutant allele for the nail genomic DNA of the mother. The reverse sequence is shown. A heterozygous 2-bp (CA) deletion corresponding to the 1317_1318delTG at exon 10 has been delineated by the direct sequencing, and confirmed by the subsequent sequencing of the subcloned normal and mutant alleles. Note that the "C" nucleotide corresponding to the "G" nucleotide that should have been dropped after the amplification with the specific forward primer (see Fig. 2) is deleted from the normal and the mutant alleles.

the leukocyte and the nail genomic DNA. Because there was no restriction enzyme that specifically digest the normal allele, a specific forward primer was designed to introduce a *Bst*XI site into the normal allele only, and nested PCR amplification followed by *Bst*XI digestion was carried out three times with different reverse primers (Fig. 2). Each run of nested PCR was performed for 35 cycles. Subsequently, sequence analysis was performed for the final PCR products from a reverse direction, delineating the 2-bp deletion mutation in the nail DNA (Fig. 1-C), while the mutation was still undetected in the leukocyte DNA. Other tissues such as hair, buccal cell swabs, and skin fibroblasts were not examined, because the mother hoped us to examine the nail as a first step, and to analyze other tissues when no mutation was identified in the nail.

Results and Discussion

The heterozygous 2-bp mutation was identified for the leukocyte DNA by the standard direct sequencing in the proband, whereas it was revealed in the nail, not leukocyte, DNA after the selective amplification of the mutant allele in the mother. Because contamination of the proband's tissue or DNA to the maternal sample was prevented as much as possible, it is likely that the 2-bp deletion mutation took place as a somatic mutation involving the germ cells in the mother and was transmitted to the proband as a germline mutation. Furthermore, the results indicate the usefulness of PCR-based selective amplification of the mutant allele and the importance to analyze plural tissues in the detection of a somatic mutation. In this regard, because the 2-bp deletion mutation was identified in the nail DNA and the mother had dental agenesis, it may relatively be prevalent in the ectodermal tissues. The mutant allele, however, would be infrequent even in the nails, because it was undetected after the standard PCR amplification. At the same time, the mutant allele, though it was identified after the nested PCR, would not be extremely rare, because the hybridization efficiency of the specific forward primer missing the "G" nucleotide would be low for both the normal and the mutant alleles (Fig. 2).

Because the 2-bp deletion mutation leads to the frameshift and resultant premature termination, it should be a loss-of-function mutation, as has been indicated in KS (4–7). Thus, clinically discernible HH, olfactory dysfunction, and dental agenesis of the proband would primarily be ascribed to the heterozygous germline mutation of *FGFR1* (4, 6, 7). For HH, although the results of the GnRH test were grossly normal, endogenous GnRH secretion would have more or less been attenuated in the proband. In this regard, the endocrine data would be consistent with the previous finding that human chorionic gonadotropin-stimulated T value is more useful than GnRH-stimulated gonadotropin value in the diagnosis of HH in prepubertal boys (12). Furthermore, the maternal fertile phenotype may be compatible with the somatic mutation, because clinical features can be mitigated by the presence of mutation negative cells in the target tissues (8). Indeed, her menarchial age and menstrual cycles remained

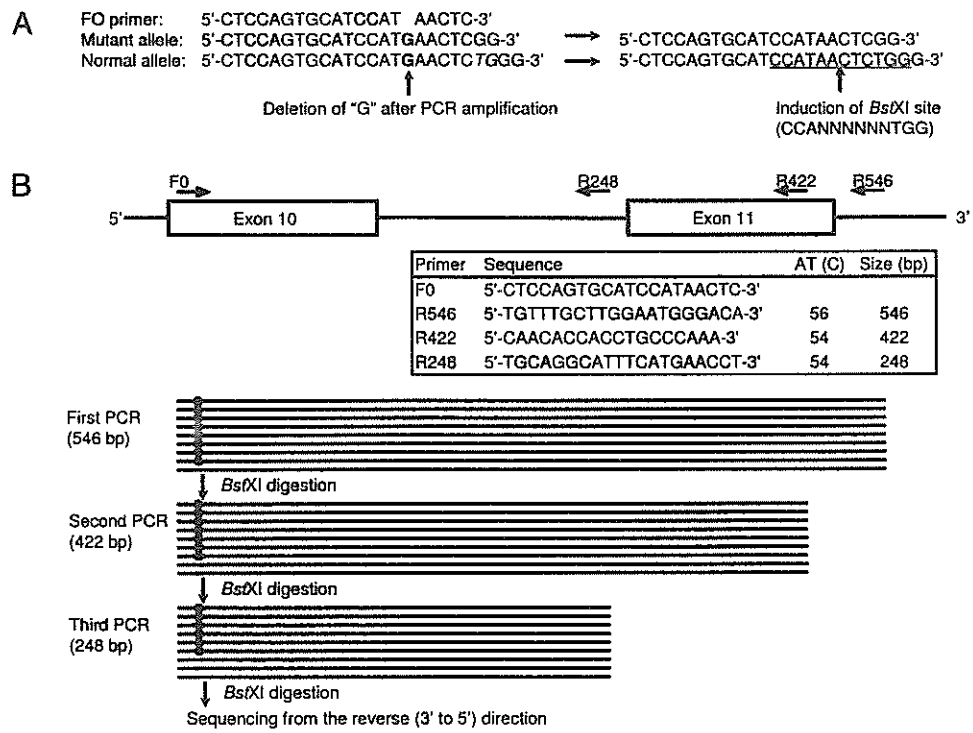

FIG. 2. The methods for the identification of the somatic mutation in the mother. A, The F0 primer sequence used for the induction of a restriction enzyme site into the normal allele preserving the "TG" nucleotide (*italicized*). The primer has been designed to drop the "G" nucleotide (*boldfaced*) after PCR amplification. As a consequence, a *Bst*XI site (*underlined*) is created in the normal allele, but not in the mutant allele. B, The selective amplification of the mutant allele in the mother. The amplification consists of three steps: 1) the first PCR with F0 and R546 primers for the genomic DNA, followed by the *Bst*XI digestion; 2) the second PCR with F0 and R422 primers for the products of the first PCR, followed by the *Bst*XI digestion; and 3) the third PCR with F0 and R248 primers for the products of the second PCR, followed by the *Bst*XI digestion. Consequently, the normal allele (shown as *horizontal lines*, with *dots* indicating the *Bst*XI site) is gradually eliminated, and the mutant allele (shown as *horizontal lines without dots*) is gradually amplified. The final products have been sequenced from the reverse direction. The sequence of each primer is shown in the *box*, together with the annealing temperature (AT) and the product size.

within the normal range, while it is uncertain whether her prolonged postpartum amenorrheic periods are related to the somatic mutation. However, the phenotypic spectrum in germline *FGFR1* mutation positive patients is known to be variable, including the typical KS phenotype, olfactory dysfunction only phenotype, and apparently normal phenotype (4–7). In addition, FGFR1 and anosmin-1 encoded by *KAL1* are likely to interact in FGF signaling involved in the development of olfactory bulbs (the target regions in KS) (4, 6, 13), and the local concentration of anosmin-1 should be higher in females than in males, because *KAL1* partially escapes X-inactivation (3). Such a wide phenotypic variability and an advantageous factor in females may also account for the preserved fertility in the mother.

The present data would provide a useful implication for the molecular diagnosis. To date, *FGFR1* mutations have not been identified in several KS patients with cleft palate and/or dental agenesis (5). Such patients might also have somatic mutations of *FGFR1* that could not be detected in leukocyte DNA by the standard sequencing method.

Acknowledgments

Received October 12, 2005. Accepted January 9, 2006.

Address all correspondence and requests for reprints to: Dr. Tsutomu Ogata, Department of Endocrinology and Metabolism, National Research Institute for Child Health and Development, Tokyo 157-8535, Japan. E-mail: tomogata@nch.go.jp.

This work was supported by Child Health and Development from the Ministry of Health, Labor, and Welfare (17C-2), a grant from the Kawano Masanori Memorial Foundation for Promotion of Pediatrics, and a Grant-in-Aid for Scientific Research on Priority Areas from the Ministry of Education, Science, Sports, and Culture (16086215).

The authors have nothing to declare.

References

1. **Kallmann FJ, Schoenfeld WA, Barrera SE** 1944 The genetic aspects of primary eunuchoidism. Am J Ment Defic 48:203–236
2. **Legouis R, Hardelin JP, Levilliers J, Claverie JM, Compain S, Wunderle V, Millasseau P, Le Paslier D, Cohen D, Caterina D, Bougueleret L, Delemarre-Van de Waal H, Lutfalla G, Weissenbach J, Petit C** 1991 The candidate gene for the X-linked Kallmann syndrome encodes a protein related to adhesion molecules. Cell 67:423–435
3. **Franco B, Guioli S, Pragliola A, Incerti B, Bardoni B, Tonlorenzi R, Carrozzo R, Maestrini E, Pieretti M, Taillon-Miller P, Brown CJ, Willard HF, Lawrence C, Persico MG, Camerino G, Ballabio A** 1991 A gene deleted in Kallmann's syndrome shares homology with neural cell adhesion and axonal path-finding molecules. Nature 353:529–536
4. **Dodé C, Levilliers J, Dupont JM, De Paepe A, Le Du N, Soussi-Yanicostas N, Coimbra RS, Delmaghani S, Compain-Nouaille S, Baverel F, Pecheux C, Le Tessier D, Cruaud C, Delpech M, Speleman F, Vermeulen S, Amalfitano A, Bachelot Y, Bouchard P, Cabrol S, Carel JC, Delemarre-van de Waal H, Goulet-Salmon B, Kottler ML, Richard O, et al** 2003 Loss-of-function mutations in FGFR1 cause autosomal dominant Kallmann syndrome. Nat Genet 33:463–465
5. **Sato N, Katsumata N, Kagami M, Hasegawa T, Hori N, Kawakita S, Minowada S, Shimotsuka A, Shishiba Y, Yokozawa M, Yasuda T, Nagasaki K, Hasegawa D, Hasegawa Y, Tachibana K, Naiki Y, Horikawa R, Tanaka T, Ogata T** 2004 Clinical assessment and mutation analysis of Kallmann syndrome 1 (KAL1) and fibroblast growth factor receptor 1 (FGFR1, or KAL2) in five families and 18 sporadic patients. J Clin Endocrinol Metab 89:1079–1088
6. **Dodé C, Hardelin JP** 2004 Kallmann syndrome: fibroblast growth factor signaling insufficiency? J Mol Med 82:725–734
7. **Albuisson J, Pecheux C, Carel JC, Lacombe D, Leheup B, Lapuzina P, Bouchard P, Legius E, Matthijs G, Wasniewska M, Delpech M, Young J, Hardelin JP, Dode C** 2005 Kallmann syndrome: 14 novel mutations in KAL1 and FGFR1 (KAL2). Hum Mutat 25:98–99
8. **Zlotogora J** 1998 Germ line mosaicism. Hum Genet 102:381–386
9. **Belsey EM, Pinol AP** 1997 Menstrual bleeding patterns in untreated women. Task force on long-acting systemic agents for fertility regulation. Contraception 55:57–65
10. **Glasier A, McNeilly AS** 1990 Physiology of lactation. Baillieres Clin Endocrinol Metab 4:379–395
11. **Tanigawara Y, Kita T, Hirono M, Sakaeda T, Komada F, Okumura K** 2001 Identification of *N*-acetyltransferase 2 and CYP2C19 genotypes for hair, buccal cell swabs, or fingernails compared with blood. Ther Drug Monit 23:341–346
12. **Dunkel L, Perheentupa J, Virtanen M, Maenpaa J** 1985 Gonadotropin-releasing hormone test and human chorionic gonadotropin test in the diagnosis of gonadotropin deficiency in prepubertal boys. J Pediatr 107:388–392
13. **Gonzalez-Martinez D, Kim SH, Hu Y, Guimond S, Schofield J, Winyard P, Vannelli GB, Turnbull J, Bouloux PM** 2004 Anosmin-1 modulates fibroblast growth factor receptor 1 signaling in human gonadotropin-releasing hormone olfactory neuroblasts through a heparan sulfate-dependent mechanism. J Neurosci 24:10384–10392

GENETIC TESTING
Volume 10, Number 4, 2006

00-0000

AU1

Screening for Partial Deletions in the *CREBBP* Gene in Rubinstein-Taybi Syndrome Patients Using Multiplex PCR/Liquid Chromatography

TORU UDAKA,[1] KENJI KUROSAWA,[2] KOSUKE IZUMI,[1] SHINOBU YOSHIDA,[3] MASATO TSUKAHARA,[4] NOBUHIKO OKAMOTO,[5] CHIHARU TORII,[1] RIKA KOSAKI,[6] MITSUO MASUNO,[2] NOBORU HOSOKAI,[7] TAKAO TAKAHASHI,[1] and KENJIRO KOSAKI[1]

ABSTRACT

Rubinstein–Taybi syndrome (RTS, MIM 180849) is a multiple malformation syndrome characterized by growth retardation, evelopmental delay, and dysmorphic features, including down-slanting palpebral fissures, a beaked nose, broad thumbs, and halluces. Mutations in the gene encoding the *CREB-binding protein* gene (*CREBBP*, also known as *CBP*) on chromosome 16p13.3 were identified in 1995. Recently, we developed a mutation analysis protocol using denaturing high-performance liquid chromatography (DHPLC) and identified heterozygous *CREBBP* mutations in 12 of 21 RTS patients. To test whether exonic deletions represent a common pathogenic mechanism, we assessed the copy number of all the coding exons using a recently developed method, the multiplex PCR/liquid chromatography assay (MP/LC). By using MP/LC, we performed screening for *CREBPP* exonic deletions among 25 RTS patients in whom no point mutations or small insertions/deletions were identified by DHPLC screening. We identified four classic RTS patients with deletions encompassing multiple exons (14–16, 5–31, 1–16, and 4–26). We conclude that large deletions including several exons are a relatively frequent cause of RTS, and that MP/LC is an effective method for detecting these deletions.

INTRODUCTION

RUBINSTEIN–TAYBI SYNDROME (RTS, MIM 180849) is a multiple malformation syndrome characterized by growth retardation, developmental delay, and dysmorphic features, including down-slanting palpebral fissures, a beaked nose, broad thumbs, and halluces (Rubinstein and Taybi 1963). Mutations in the gene encoding the *CREB-binding protein gene* (*CREBBP*, also known as *CBP*) on chromosome 16p13.3 were identified in 1995 (Petrij *et al.* 1995). Large deletions involving the *CREBBP* gene, detected by fluorescence in situ hybridization (FISH) analysis, account for about 10% of RTS cases (Blough *et al.* 2000; Petrij *et al.* 2000)

Recently, we developed a mutation scanning system based on denaturing high-performance liquid chromatography (DHPLC)-heteroduplex analysis (O'Donovan *et al.* 1998; Kosaki *et al.* 2005) to detect exon(s) that may harbor mutations prior to performing a sequencing analysis. Using this system, we identified heterozygous *CREBBP* mutations in 12 of 21 RTS patients (57%). The mutation detection rate of our DHPLC-heteroduplex analysis was comparable to that recently reported by Bartsch *et al.*, who performed PCR-sequencing of all the exons (Bartsch *et al.* 2005; Udaka *et al.* 2005). Bartsch *et al.* (2005) suggested that RTS might be a genetically heterogeneous disorder and that RTS could be caused by gene(s) other than *CREBBP* in up to 30% of cases. Their inference was partly sup-

[1]Department of Pediatrics, Keio University School of Medicine, Tokyo, Japan.
[2]Division of Medical Genetics, Kanagawa Children's Medical Center, Yokohama, Japan.
[3]Department of Pediatrics, Omihachiman City Hospital, Shiga, Japan.
[4]Faculty of Health Sciences, Yamaguchi University School of Medicine, Ube, Japan.
[5]Department of Planning and Research, Osaka Medical Center and Research Institute for Maternal and Child Health, Osaka, Japan.
[6]Department of Clinical Genetics and Molecular Medicine, National Children's Medical Center, Tokyo, Japan.
[7] Research and Development Division, Mitsubishi Kagaku Bio-Clinical Laboratory, Tokyo, Japan.

ported by the identification of an *EP300* mutation in some (~3%) patients with RTS (Roelfsema *et al.* 2005). However, the pathogenic mechanisms in the remaining cases were not determined. Possible mechanisms include deletion of one or more exons in the *CREBBP* gene, because our study and that by Bartsch *et al.* relied on DHPLC-based heteropuplex analysis and PCR sequencing, respectively, neither of which allows the detection of this type of mutation (Bartsch *et al.* 2005; Udaka *et al.* 2005).

To test whether exonic deletions represent a common pathogenic mechanism, we assessed the copy number of all the coding exons using a recently developed method, the multiplex PCR/liquid chromatography assay (MP/LC) (Dehainault *et al.* 2004). First, a multiplex PCR with unlabeled primers enables simultaneous amplification of multiple exons under semiquantitative conditions. Second, PCR products are separated by nondenaturing ion-pair reversed-phase HPLC and, lastly, are quantitated by fluorescent detection using a post-column intercalation dye. The relative peak intensities for each target directly reflect exon copy number. Using MP/LC, we screened for *CREBBP* exonic deletions among 25 RTS patients, in whom no point mutations or small insertions/deletions had been identified by DHPLC-based heteroduplex analysis. As a result, we found 4 RTS patients who had deletions encompassing various portions of the *CREBBP* gene.

MATERIALS AND METHODS

Patients

Genomic DNAs from 47 Japanese patients who had been clinically diagnosed as having RTS were analyzed. The criteria for enrollment included down-slanting palpebral fissures, a beaked nose, broad thumbs or broad halluces, and developmental delay. All of the patients were unrelated and were sporadic cases. The patients and their family members were enrolled in the study after providing their written informed consent, according to a protocol approved by our institution's review board. Mutation analysis in a subset (*i.e.*, 21 of 47 patients) had been published elsewhere (Udaka *et al.* 2005). Among the 47 patients, 11 had been screened for large deletions using FISH with a cosmid RT1 (D16S237) probe specific to the 3′ region of *CREBBP* (exons 20–31) (Breuning *et al.* 1993; Masuno *et al.* 1994); no deletions were identified.

Genomic DNA was isolated using the QIAamp system (Qiagen Inc. Valencia, CA). The concentration of DNA in each sample was determined using a Nanodrop ND-1000 spectrophotometer (NanoDropTechnologies, Wilmington, DE). Screening for point mutations and small insertions/deletions in the *CREBBP* gene was performed using DHPLC, as described elsewhere (Udaka *et al.* 2005).

Copy number scanning using the MP/LC assay

Twenty two patients who had point mutations and small insertions/deletions in *CREBBP* were excluded from further studies (see Supplemental Table 1; available at http://www.dhplc.jp/). The remaining 25 patients were further analyzed using the MP/LC assay (Dehainault *et al.* 2004). ST1

Ten sets of multiplex PCR, including all the coding exons of the *CREBBP* gene, were performed using the primers described in Supplemental Table 2. Each multiplex PCR also included a set of primers for a control gene on a chromosome, other than chromosome 16 on which the *CREBBP* gene resides (Supplemental Table 2; available at http://www.dhplc.jp/). The use of the control gene makes the assay capable of detecting deletions of the entire *CREBBP* gene. ST2

The PCRs were performed in a volume of 20 μl containing 30 ng of genomic DNA, 5 pmol of each *CBP*-forward and -reverse primer, 5 pmol each of the reference-forward and -reverse primer, 0.2 m*M* dNTPs, 1.5 m*M* $MgCl_2$, 5% dimethylsulfoxide (DMSO), 0.5 U of AmpliTaq Gold polymerase, and the buffer supplied by the manufacturer (Applied Biosystems, Foster City, CA). Only for Multiplex 10, Platinum *Taq* polymerase high fidelity (Invitrogen, Carlsbad, CA) was used, because of the high GC content of exon 1. Cycling conditions consisted of a first denaturation step of 95°C for 10 min, followed by 25 cycles of denaturation at 95°C for 30 sec, annealing at 58°C for 30 sec and extension at 72°C for 30 sec, followed by a final extension at 72°C for 10 min.

Aliquots of 5 μl of multiplex PCR products were injected on a semiautomated Wave 3500HT system (Transgenomic, Omaha, NE), incorporating a high sensitivity detector (HSD). The HSD uses post-column intercalation chemistries, *i.e.*, SYBR Green 1 (Invitrogen, Carlsbad, CA), and fluorescence detection to provide sensitivity enhancement for the detection of DNA. Separation was performed using a DNAsep cartridge (Transgenomic) and a constant oven temperature of 50°C to ensure non-denaturing conditions. An elution gradient was generated by mixing Buffer A (0.1 mol/L triethylammonium acetate) and Buffer B (0.1 mol/L triethylammonium acetate containing 250 mL/L acetonitrile) in a linear gradient from the start 54.2% B to a final 63.2% B over a period of 4.5 min.

Following separation, eluted PCR products were mixed with the Wave HS Staining Solution I that contained SYBR Green 1 by using the HSX accessory, and were then detected with the FDX fluorescence detector (Transgenomic). Data were ana-

FIG. 1. MP/LC chromatograms of Patient 4 obtained with complete 10 sets of multiplex PCR from *CREBBP* exon 1 to exon 31. *x*-axis, retention time in min; *y* axis, fluorescence intensity. Exons under study are indicated at the tops of the corresponding peaks. The chromatograms in black and red represent the normal control and the patient, respectively. Profiles are superimposed and then normalized using the reference amplicon (*CHD7* gene on chromosome 8q or *TCOF1* gene on chromosome 5q, indicated as "C"). Exons 4–26 were deleted.

FIG. 2. MP/LC chromatograms of Patients 1, 2, and 3 for selected sets of multiplex PCR from *CREBBP* exon 1 to exon 31. *x* axis, retention time in min; *y* axis, fluorescence intensity. Exons under study are indicated at the tops of the corresponding peaks. The chromatograms in black and red represent the normal control and the patient, respectively. Profiles are superimposed and then normalized using the reference amplicon (*CHD7* gene on chromosome 8q or *TCOF1* gene on chromosome 5q, indicated as "C"). Exons 14–16 of Patient 1, exons 5–31 of Patient 2, and exons 1–16 of Patient 3 were deleted.

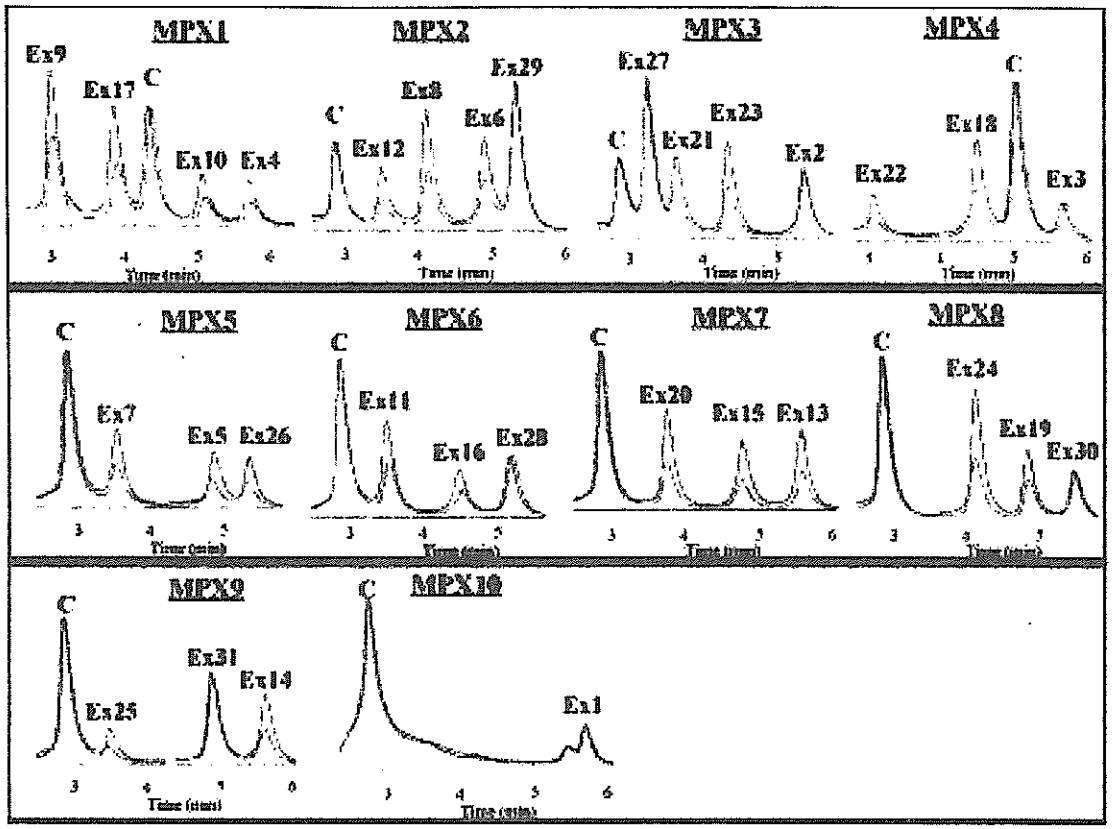

4C

FIG. 1.

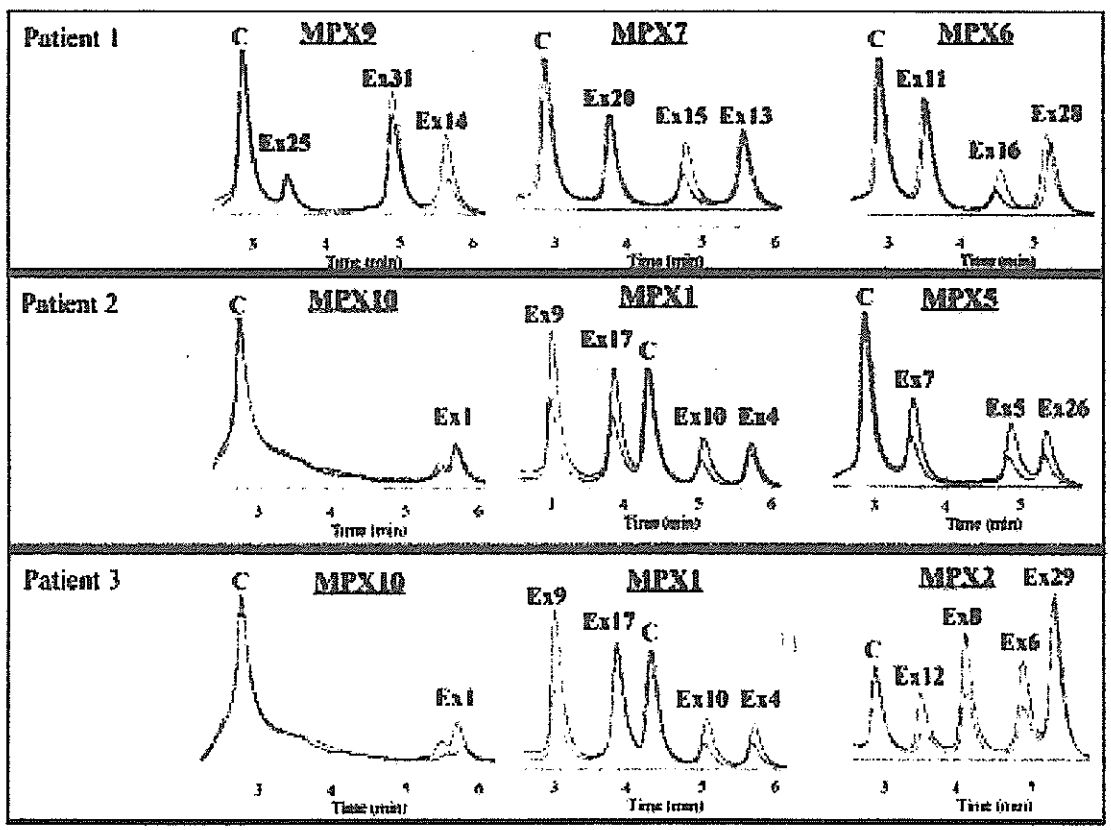

4C

FIG. 2.

lyzed using Navigator 1.5.3 software (Transgenomic). Briefly, chromatograms from patients were superimposed onto those of several normal controls. The relative fluorescence intensities between the patient and normal controls were normalized using the control gene peak as a reference.. The yield of each amplicon in each patient sample was evaluated and a deletion was indicated by a two-fold decrease in the corresponding peak.

FISH

Two of the deletions detected by the MP/LC assay were confirmed by FISH using probes designed to detect particular deletions. The FISH probes were prepared by long-range PCR using genomic DNA from a normal control individual. For a probe spanning exons 14–16 (CBP_14_16) a 6.5-kb amplicon was prepared using primer set CBP_FISH_2F (5′- catttt-caaacgggggaaat -3′, within intron 13) and CBP_FISH_2R (5′-gagccactgtgtccactcat -3′, within intron 16). For a probe spanning exons 17–19 (CBP_17_19) a 6.2-kb amplicon was prepared using primer set CBP_FISH_1F (5′-ttgcctcacaagct-gaacac-3′, within intron 16) and CBP_FISH_1R (5′-tgga-tcacacaagcgagaag-3′, within intron 19).

RESULTS

The *CREBBP* locus was screened in 10 multiplex reactions (Supplemental Table 2). Primer combinations were optimized to meet the following criteria: (1) amplicon sizes are sufficiently different so that each amplicon would be successfully separated by HPLC and (2) amplification efficiencies are comparable. After several optimization trials, we found that at least 10-bp differences were required for successful separation (Fig. 1).

F1

MP/LC screening identified 4 RTS patients with large deletions among 25 patients in whom DHPLC screening (Udaka *et al.* 2005) did not reveal point mutations or small insertions/deletions in the *CREBBP* gene (Figs. 1 and 2).

F2

Patient 1

A Japanese girl was born at 41 weeks of gestation. The patient's birth weight was 3,074 g. Characteristic facial features included a narrow, hairy forehead, long eyelashes, synophrys, posteriorly rotated low-set ears, anteverted nares, long philtrum, a thin upper lip with a downturned mouth, micrognathia, and a short neck. Remarkable upper limb characteristics included broad thumbs. The patient could not follow objects across midline at 5 months of age. On the basis of these characteristic features, we diagnosed the patient as having RTS. Chromosomes were 46,XX, inv(9)(p12q13).

MP/LC screening revealed exons 14–16 to be deleted, whereas exons 1–13 and exons 17–31 were not (Fig. 2). The deletion was confirmed with FISH using a probe, CBP_14_16, prepared to detect this deletion. The FISH probe hybridized to only one of the two homologous chromosome 16 regions (Fig. 3).

F3

To define the deletion more precisely, we performed long-range PCR using primers from exon 13 (ex13F) and exon 17 (ex17R) (Fig. 4). In the patient specimen, a 4.5-kb PCR fragment was generated by primers ex13F and ex17R, which are 15.2 kb apart on the wild-type allele (see Fig. 6, below). The deletion involved 10,916 bp from intron 13 (IVS13-342) to intron 16 (IVS16+7306) and results in loss of exons 14–16. The deletion would lead to a frameshift and premature stop codon 15 codons after codon 821 (the last codon of exon 13).

F4

Patient 2

A Japanese boy was born at term after an uncomplicated delivery. The pregnancy was remarkable for polyhydramnios, first noted at 26 weeks of gestation. The patient's birth weight was 2,602 g, and his body length was 46.5 cm. Characteristic facial features included a narrow, hairy forehead, long eyelashes, synophrys, posteriorly rotated low-set ears, anteverted nares, long philtrum, a thin upper lip with a downturned mouth, micrognathia, and a short neck. The patient also exhibited bilateral broad thumbs and bilateral cryptorchidism. Based on these characteristic features, we diagnosed the patient as having RTS. His chromosomes were normal. An echocardiogram revealed hypoplastic left heart syndrome. Unfortunately, he acquired a severe infection and died of multiple organ failure at 3 months of age.

MP/LC screening revealed exons 5–31 to be deleted, whereas exons 1–4 were not (Fig. 2). The deletion would lead to protein truncation.

Patient 3

A Japanese girl was born at term after an uncomplicated pregnancy and delivery. The patient's birth weight was 2,495 g, and her body length was 42 cm. Characteristic facial features included a narrow, hairy forehead, long eyelashes, synophrys, posteriorly rotated low-set ears, anteverted nares, long philtrum, a thin upper lip with a downturned mouth, micrognathia, and a short neck.

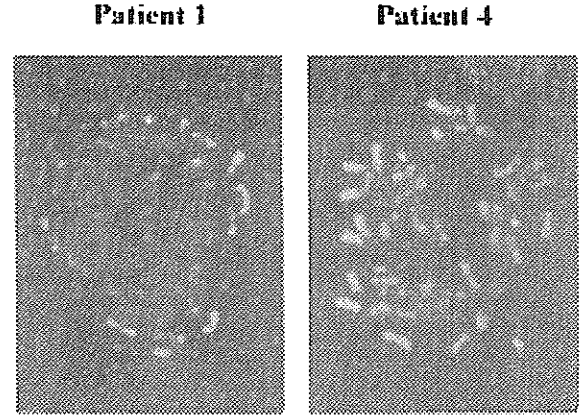

FIG. 3. FISH analysis of the deletion. **Left:** Metaphase spreads of the Patient 1 revealed a deletion in one of the chromosome 16 homologs when hybridized with a probe prepared by long-range PCR of *CREBBP* exons 14–16 from a normal control individual (red signal) and chromosome 16 centromere probes (green signals). **Right:** Metaphase spreads of the Patient 4 revealed a deletion in one of the chromosome 16 homologs when hybridized with a probe prepared by long-range PCR of *CREBBP* exons 17–19 from a normal control individual (red signal) and chromosome 16 centromere probes (green signals).

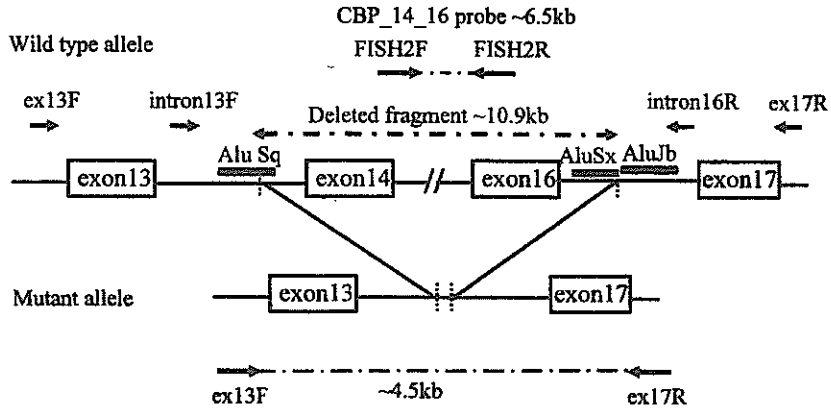

FIG. 4. Breakpoint cloning in Patient 1. Patient 1 has a deletion of exons 14–16 of the *CREBBP* gene. The figures shows the PCR strategy for the amplification of the deleted allele. *CREBBP* exons 13–17 (not drawn to scale) are boxed and numbered; introns are indicated by solid lines. F and R indicate forward and reverse primers, respectively. The figure also shows the approximate positions of repetitive sequences near the breakpoints of the deletion (Alu Sq, Alu Sx, Alu Jb).

The patient had bilateral broad thumbs and toes. On the basis of these characteristic features, we diagnosed the patient as having RTS. Her neck remained unstable at 5 months of age, and she was unable to follow objects across the midline.

MP/LC screening revealed the deletion of exons 1–16, although exons 17–31 were intact (Fig. 2). The deletion led to loss of the start codon, and no protein was translated from the mutant allele.

Patient 4

This patient had typical facial features and broad thumbs. Unfortunately, no further clinical data were available. MP/LC screening revealed the deletion of exons 4–26, although exons 1–3 and exons 27–31 were intact (Fig. 1). The deletion was confirmed with FISH using a probe, CBP_17_19, designed to detect this deletion. The FISH probe hybridized to only one of the two homologous chromosome 16 regions (Fig. 3).

To define the deletion more precisely, we performed long-range PCR using primers from exon 3 (ex3F) and exon 28 (ex28R) (Fig. 5). In the patient specimen, a 12-kb PCR fragment was generated by primers ex3F and ex28R, which are 75 kb apart on the wild-type allele (Fig. 6). The deletion involved 61,640 bp from intron 3 (IVS3+10556) to intron 26 (IVS26+149) and results in loss of exons 4–26. The sequence at the junction created by the deletion is shown in Fig. 6. The deletion would lead to a frameshift and premature stop codon 13 codons after codon 325.

F5

F6

DISCUSSION

The analysis of copy number aberrations, especially deletions, is a major focus of interest in mutation analyses of multiple malformation syndromes (Armour *et al.* 2002), because commonly used techniques such as direct sequencing cannot

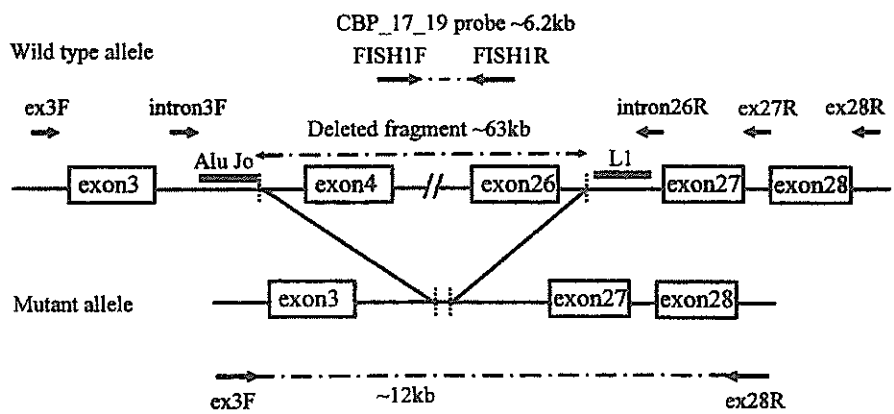

FIG. 5. Breakpoint cloning in Patient 4. Patient 4 has a deletion of exons 4–26 of the *CREBBP* gene. The figures shows the PCR strategy for the amplification of the deleted allele. *CREBBP* exons 3–28 (not drawn to scale) are boxed and numbered, introns are indicated by solid lines. F and R indicate forward and reverse primers, respectively. The figure also shows the approximate positions of repetitive sequences near the breakpoints of the deletion (Alu Jo, L1).

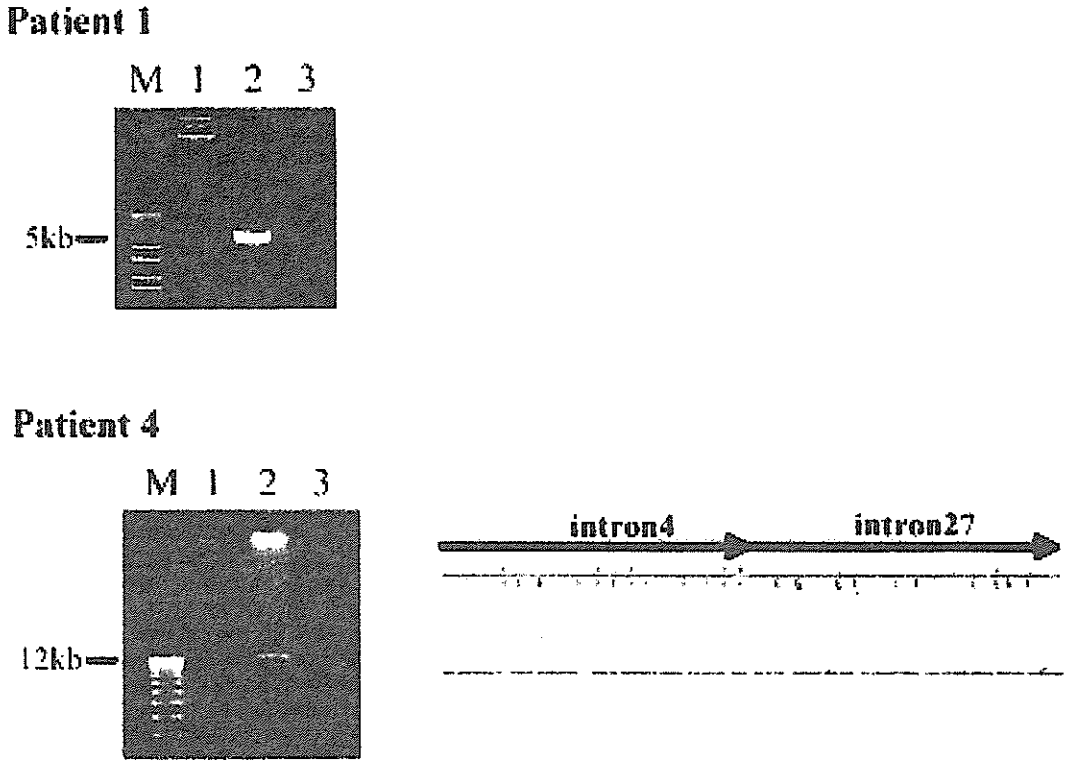

FIG. 6. Analysis of the junctional fragments. **Top:** Junctional fragment amplified by long-range PCR from patient 1 using primers exon13F and exon17R as shown in Fig. 4. **Lane M:** 1-kb ladder. **Lane 1:** normal control. **Lane 2:** patient 1. **Lane 3:** negative control. A 4.5-kb product was observed for Patient 1's mutant allele (lane 2), whereas no product was amplified from the normal control (lanes 1) because primers exon13F and exon17R are too far apart (15.2 kb) in the wild-type allele. **Bottom, left:** Junctional fragment amplified by long-range PCR from Patient 4 using primers exon3F and exon28R as shown in Fig. 5. **Lane M:** 1-kb ladder. **Lane 1:** normal control. **Lane 2:** Patient 4. **Lane 3:** negative control. A 12-kb product was observed from Patient 4's mutant allele (lane 2), whereas no product was amplified from the normal control (lane 1) because primers ex3F and ex28R are too far apart (75-kb) in the wild-type allele. **Bottom, right:** Sequencing chromatogram across the junction created by the deletion using the 12-kb long-range PCR product as template, and the intron3F and intron26R oligos (Fig. 5) as sequencing primers.

detect this class of mutations. Hence, the development of an assay system to detect this class of mutations is critical. Indeed, the prevalence of such mutations will never be appreciated until it is appropriately surveyed. In the present study, we developed a MP/LC-based assay that enables the copy number of all the coding exons of *CREBBP* to be assessed. This assay allowed us to identify interstitial deletions in 4 patients with RTS. Overall, the sensitivity of the *CREBBP* mutation analysis increased from 47% (22/47) to 55% (26/47) with the introduction of the MP/LC assay.

The assay reported herein represents the first comprehensive deletion detection system that covers all the coding exons of *CREBBP*. Previously, a FISH assay using multiple cosmid probes (Petrij *et al.* 2000) or a multiplex ligation-dependent probe amplification (MLPA) assay (Roelfsema *et al.* 2005) using probes corresponding to selected exons were used to screen for partial deletions of the *CREBBP* locus. The present MP/LC system provides sufficient resolution to determine rearrangements down to the level of individual exons. Furthermore, with the help of MP/LC, we were able to delineate the breakpoints at the nucleotide sequence level in 2 patients with exonic deletions within the *CREBBP* locus.

As for the two deletion events characterized in patients 1 and 4, the exact underlying mechanism responsible for the instability is not known. In patient 1, an *Alu–Alu*-mediated recombination event may have played a role in the genomic rearrangements in that *Alu* sequences were present at the deletion breakpoints. In Patient 4, it is intriguing to note that both the proximal and distal breakpoints were localized near repeat sequences: The deletion breakpoint in intron 3 was localized near an *Alu* element and the breakpoint in intron 26 was also in a region flanking an L1 element. An additional adenine nucleotide was added at the deletion junction. Taking these features into account, we suspect that nonhomologous end joining (Roth and Wilson 1986; Shaw and Lupski 2004) may have played a role in the creation of this mutation.

Theoretically speaking, MP/LC should be capable of determining the copy number of any locus or of any exon within a locus in the genome, as long as the target sequence is unique within the genome. Consequently, MP/LC is a very useful as-